Optimal and Maximized Configurable Power Saving Protocols for Corona-Based Wireless Sensor Networks

Yu-Hsiang Lin, Zi-Tsan Chou, *Member, IEEE*, Chun-Wei Yu, and Rong-Hong Jan

Abstract—Wireless sensor networks (WSNs) are one of the most important ingredients in the Internet of Things. Thus it is vital to design a good power saving protocol, which operates at the medium access control (MAC) layer, for a WSN since sensors are generally battery-powered. On the other hand, organizing a WSN into coronas centered at the sink is a simple effective technique to achieve low-overhead routing where every sensor needs neither to broadcast beacons nor to maintain routing/neighbor tables. Hence in this paper, we propose an optimal and maximized configurable power saving protocol, named Green-MAC, for a corona-based WSN, which has the following attractive features. (i) By using the generalized Chinese remainder theorem, Green-MAC guarantees that any two sensors in the neighboring coronas can simultaneously wake up in bounded time regardless of their schedule offset as well as their respective cycle lengths. (ii) Given the cycle length, the ATF-ratio (i.e. the fraction of awake time frames in a cycle) of each sensor reaches the theoretical minimum. (iii) Under the minimum ATF-ratio constraints, the number of configurable ATF-ratios of each sensor reaches the theoretical maximum. (iv) An ATF-ratio configuration scheme is proposed for Green-MAC such that the power consumption of a WSN can be minimized while the worst event-to-sink delay requirement can be fulfilled with high probability. Both theoretical analysis and simulation results demonstrate that Green-MAC greatly outperforms existing power saving protocols for corona-based WSNs, including Q-MAC and Queen-MAC, in terms of ATF-ratio, configurability, network lifetime, delay violation ratio, and event-to-sink throughput.

Index Terms—Chinese remainder theorem, medium access control (MAC), power saving protocol, quorum, and wireless sensor network (WSN)

1 Introduction

Wireless sensor networks (WSNs) are expected to play a significant role in the future Internet of Things [2] due to their advantages in supporting applications requiring quick and low-cost deployment. In a WSN, a large number of *sensors* capable of sensing, processing, and wireless transmission are scattered in a region of interest, and collaborate to report the sensed information to the *sink* through a multi-hop fashion to achieve a certain common goal [1], [19]. Since sensors are generally powered by batteries, it is essential to design a good power saving protocol, which operates at the *medium access control* (MAC) layer, to prolong the lifetime of a WSN.

1.1 Related Work

Existing power saving protocols for WSNs could be divided into two categories [1], [28]: *outband* and *inband*. In outband power saving protocols [23], [25], all sensors are equipped with two radios: data radio and wakeup radio, where these two radios operate in different channels. The data radio keeps sleeping until communication is desired, while the wakeup radio periodically wakes up for a short time to listen for the wakeup signal. Once the source sensor s_1 ensures that the intended receiver s_2 is awaken by its continuous signal transmitted via the wakeup channel, s_1 can employ an 802.11-like MAC to transfer data to s_2 via the data channel [23]. Obviously, the high energy efficiency of the outband power saving protocols comes at the expense of extra hardware cost as compared with the inband ones.

The inband power saving protocols where each sensor is equipped with only one radio could be divided into two categories [6], [12]: *asynchronous* and *synchronous*. In asynchronous power saving protocols [4], [24], each sensor independently sets its inter-wakeup interval (e.g. 20 ms) to periodically turn on its radio to check the medium. When a sensor has data to send, it transmits a preamble that is long enough such that all of its neighbors can be awaken. Once the preamble is detected, the destination sensor stays awake to receive the data *immediately* after the preamble, and then goes to sleep after the finish of data transfer. The apparent advantage of asynchronous power saving protocols is their exemption from time synchronization. However, due to the inability to integrate with the RTS/CTS mechanism, such a preamble approach may easily suffer from the hidden terminal problem [5]. Besides, compared with synchronous protocols, such a long preamble produces excess energy consumption. Although these drawbacks can be mitigated by replacing the long preamble with a series of short

- *Z-T. Chou and C.-W. Yu are with the Department of Electrical Engineering, National Sun Yat-Sen University, Kaohsiung 804, Taiwan, Republic of China. E-mail: ztchou@mail.ee.nsysu.edu.tw, cwyu2014@gmail.com.*
- *Y.-H. Lin and R.-H. Jan are with the Department of Computer Science, National Chiao Tung University, Hsinchu 300, Taiwan, Republic of China. E-mail: yhlin.cs97g@g2.nctu.edu.tw, rhjan@cis.nctu.edu.tw.*

Manuscript received 4 Aug. 2014; revised 16 Dec. 2014; accepted 10 Feb. 2014. Date of publication 0 . 0000; date of current version 0 . 0000.
For information on obtaining reprints of this article, please send e-mail to: reprints@ieee.org, and reference the Digital Object Identifier below.
Digital Object Identifier no. 10.1109/TMC.2015.2404796

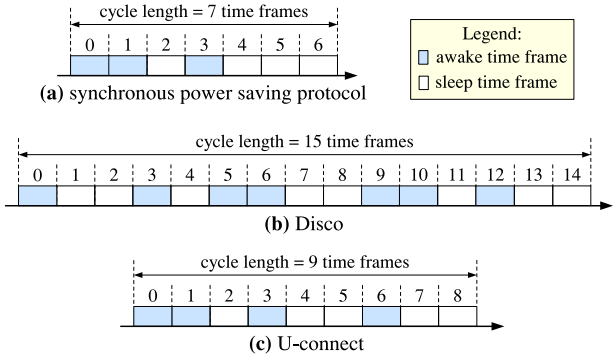

Fig. 1. Part (a) shows the cycle pattern proposed by [28]. Parts (b) and (c) respectively show the cycle patterns in Disco and U-connect when the desired ATF-ratio is about 0.5. In part (b), $p_1 = 3$ and $p_2 = 5$. In part (c), $p = 3$.

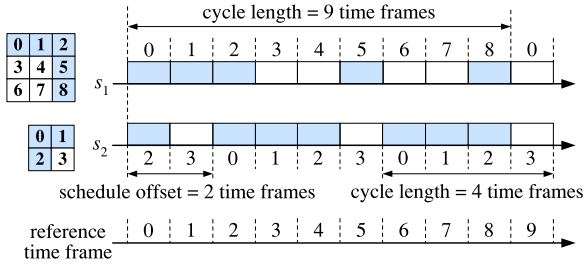

Fig. 2. An example of cycle patterns in Q-MAC, in which sensors s_1 and s_2 simultaneously wake up at the zeroth, second, and eighth reference time frames.

preamble packets [4], the authors of [6] pointed out that short preamble approach may still consume more energy when compared with synchronous protocols since more preamble packets are needed to be transmitted.

Since many WSN applications require time synchronization [10], [19], it is natural to consider synchronous (or called *rendezvous*) power saving protocols. As shown in Fig. 1a, in synchronous power saving protocols [6], [11], [12], [18], [28], time is divided into fixed-sized time frames; besides, each sensor maintains a *cycle pattern*, which specifies the positions of *awake time frames* (ATFs) and *sleep time frames* (STFs) in L consecutive time frames. We call L the *cycle length* because the specific ATF/STF pattern repeats every L time frames. Since a sensor may turn off its radio during the entire STF, synchronous power saving protocols must ensure that the source sensor and its intended receiver can simultaneously wake up in some of their ATFs for data transfer. We could further divide the synchronous power saving protocols into two categories: *non-configurable* and *configurable*. In non-configurable protocols, all sensors must adhere to the same cycle pattern [28], which implies that all sensors have the same *ATF-ratio*, which is defined as the fraction of ATFs in a cycle. Intuitively, the lower the ATF-ratio, the less frequently the sensor wakes up, the more battery power the sensor can save. On the flip side, the higher the ATF-ratio, the more frequently the sensor wakes up, the shorter data reception delay the sensor may perceive. The apparent advantage of configurable power saving protocols [6], [11], [12], [18] is that the ATF-ratio of each sensor can be configured based on the traffic load or other quality-of-service (QoS) requirements to maximize the energy efficiency. Therefore, in this paper, we focus on the configurable power saving protocols.

Disco [11], U-connect [18], Q-MAC [6], and Queen-MAC [12] are the representatives of configurable power saving protocols. In Disco [11], each sensor s individually selects an ATF-ratio ϕ and picks two primes, p_1 and p_2, where $p_1 \neq p_2$, such that the sum of $1/p_1$ and $1/p_2$ (approximately) equals ϕ. Then as depicted in Fig. 1b, in consecutive $p_1 \times p_2$ time frames indexed from 0 to $p_1 \times p_2 - 1$, the sensor s sets the time frames whose indices are divisible by p_1 or p_2 as its ATFs. In U-connect [18], each sensor s individually selects an ATF-ratio ϕ and picks a prime p such that $1.5/p$ (approximately) equals ϕ. Then as shown in Fig. 1c, in consecutive p^2 time frames indexed from 0 to $p^2 - 1$, the sensor s sets the time frames whose indices are smaller than $\lceil (p+1)/2 \rceil$ or divisible by p as its ATFs. The authors of [18] have formally shown that given a cycle length L, the ATF-ratios of Disco and U-connect are about $2/\sqrt{L}$ and $1.5/\sqrt{L}$, respectively. On the other hand, in Disco and U-connect, every sensor needs to broadcast a beacon specifying its cycle pattern in the beginning of each ATF. By Chinese remainder theorem [9], we can ensure the overlapping of ATFs between neighboring sensors. Once a sensor s_1 received a beacon from its neighbor s_2, s_1 thus discovered s_2 and can accordingly predict the ATFs of it neighbor (s_2) for data transmission. These imply that Disco and U-connect are optimized for *unicast* traffic. However, the authors of [6], [20] have shown that in a *corona-based* WSN, as depicted in Fig. 3, local traffic is mainly *anycast*; hence on the basis of this principle, the authors of [6], [12] designed *beacon-free* power saving protocols where each sensor needs not to spend memory/energy on dealing with beacon-related operations.

Quorum systems [15] have been recently utilized to design beacon-free configurable power saving protocols, including Q-MAC [6] and Queen-MAC [12]. As shown in Fig. 2, in Q-MAC, the consecutive L time frames are arranged as a $\sqrt{L} \times \sqrt{L}$ grid in a row-major fashion, where $\sqrt{L}$ is an integer. Each sensor selects one row and one column from a grid of pre-configured size $\sqrt{L} \times \sqrt{L}$ as its ATFs, while the residuals are STFs. For example, in Fig. 2, sensor s_1 sets $L = 9$ and the ith time frames, where $i \in \{0, 1, 2, 5, 8\}$, as its ATFs. By grid-quorum property [15], Q-MAC ensures that the ATFs of any two neighboring sensors can overlap regardless of their schedule offset and individual cycle

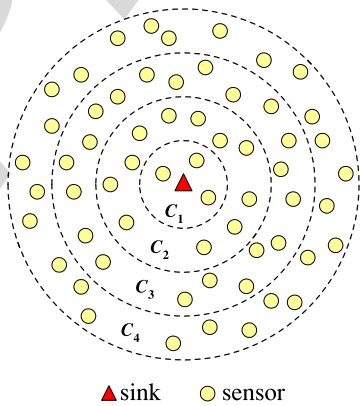

Fig. 3. Illustration of a corona-based WSN. Note that, in Q-MAC [6] and Queen-MAC [12], sensors in the ith corona, denoted by C_i, are i hops away from the sink.

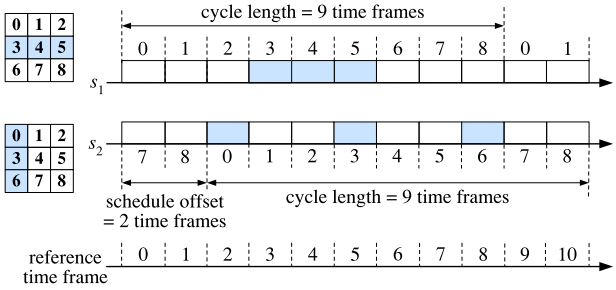

Fig. 4. An example of cycle patterns in Queen-MAC, in which sensors s_1 and s_2 in different but adjacent coronas wake up simultaneously at the fifth reference time frame.

lengths. Thus we can conclude that (i) given a cycle length L, the ATF-ratio of Q-MAC is about $2/\sqrt{L}$, which is, however, larger than that of U-connect, and (ii) given the maximum cycle length $L_{\max}$, the number of configurable ATF-ratios of each sensor is $\sqrt{L_{\max}}$. To demonstrate the power of configurability, Q-MAC operates on a corona-based WSN such that each sensor can configure its ATF-ratio according to its *corona-tier* and traffic load.

Recently, the authors of [12] further indicated that in a corona-based WSN, there is *no* need to insist on the overlap of ATFs between *every pair* of sensors. By only guaranteeing the overlap of ATFs between sensors in neighboring coronas, the whole WSN can still function well since each sensor needs to rely on merely the sensors in the inner adjacent corona to relay data to the sink. On the basis of this principle, the authors of [12] proposed a configurable power saving protocols, called Queen-MAC, in which the ATF-ratio of each sensor can achieve only *half* of that in Q-MAC. Specifically, in Queen-MAC, all sensors have the *same* cycle length L, where $\sqrt{L}$ is an integer. The consecutive L time frames are arranged as a $\sqrt{L} \times \sqrt{L}$ grid in a row-major fashion. As shown in Fig. 4, a sensor in an odd-tier corona can select i columns from the grid as its ATFs, while a sensor in an even-tier corona can select j rows from the grid as its ATFs, where $1 \leq i, j \leq \sqrt{L}$ are configurable parameters. Since rows and columns in a grid have intersections, Queen-MAC ensures the overlap of ATFs between sensors in neighboring coronas. However, we observe that, in Queen-MAC, given a cycle length L, (i) the ATF-ratio of a sensor is at least $1/\sqrt{L}$, which is still far from the optimal value, and (ii) the number of configurable ATF-ratios of each sensor is only $\sqrt{L}$. Intuitively, the larger the number of configurable ATF-ratios, the more precisely the sensors are able to configure their wakeup frequencies according to QoS requirements to achieve high energy efficiency.

1.2 Objective and Contributions

Given the maximum cycle length $L_{\max}$, let us denote the number of configurable ATF-ratios of each sensor by $\theta(L_{\max})$. We say that a configurable power saving protocol for a corona-based WSN is *optimal* and *maximized configurable* if it satisfies the following two requirements.

- **R1.** *Minimum ATF-ratio requirement*. The ATF-ratio of every sensor with a cycle length L is only $O(1/L)$.
- **R2.** *Maximized configurability requirement*. Under the constrain of **R1**, $\theta(L_{\max}) = \Omega(L_{\max}/\ln L_{\max})$.

The reasons for **R1** are that there should be at least one ATF in a cycle, and we allow that the ATFs of two neighboring sensors located in the same corona can *never* overlap. The reason for **R2** is because under the constraint of **R1**, $\Omega(L_{\max}/\ln L_{\max})$ is currently the best known asymptotic bound[1] of $\theta(L_{\max})$. (See Section 3.)

The major objective of this paper is to design a beacon-free configurable power saving protocol that satisfies both **R1** and **R2** for a corona-based WSN. The overall contributions of this paper are as follows:

- The authors of [15], [28] have proved that in *any quorum-based* power saving protocols, the ATF-ratio of a sensor with a cycle length L can be no less than $1/\lceil\sqrt{L}\rceil$. Therefore, in this paper, instead of adopting quorum systems, we employ the *generalized Chinese remainder theorem* [9] to construct the cycle pattern such that the ATF-ratio of every sensor with a cycle length L can reach the theoretical lower bound $O(1/L)$. We name our protocol *Green-MAC*. To the best of our knowledge, Green-MAC is the first configurable power saving protocol for a WSN where the ATF-ratio of *every* sensor can be much lower than the traditional quorum bound, $1/\lceil\sqrt{L}\rceil$.
- Then we prove that the number of configurable ATF-ratios in Green-MAC is asymptotically maximized. To illuminate the power of configurability, we focus the WSN applications on *event detection and reporting* [20], [25], such as intruder detection and the detection of fire and hazards. This kind of applications exhibits prolonged periods of inactivity till the time an event of interest is detected. Importantly, upon detecting an event, a report of this event has to be *promptly* relayed to the sink. To achieve this goal, we propose an ATF-ratio configuration scheme such that the power consumption of a WSN is minimized, while the worst event-to-sink delay requirement can be satisfied with a pre-specified probability.
- Finally, we evaluate the average power consumption of a WSN. We validate our analysis through simulations. Further, by conducting extensive simulations, we quantitatively show that under the architecture of a corona-based WSN, Green-MAC is much more energy-efficient than existing beacon-free configurable power saving protocols, including Q-MAC [6] and Queen-MAC [12].

The rest of this paper is organized as follows. In Section 2 and Section 3, we present and analysis the Green-MAC protocol in detail. Section 4 presents the ATF-ratio configuration scheme and analyzes the average power consumption of a WSN running Green-MAC. Extensive simulations are conducted in Section 5. Section 6 concludes this paper.

2 The Green-MAC Protocol

Green-MAC consists of four components: an initial configuration procedure, a wakeup/sleep schedule scheme, an

1. Given two functions $f(n)$ and $g(n)$, we denote $f(n) = \Omega(g(n))$ if there exists two positive constants c and n_0 such that $cg(n) \leq f(n)$ for all $n \geq n_0$.

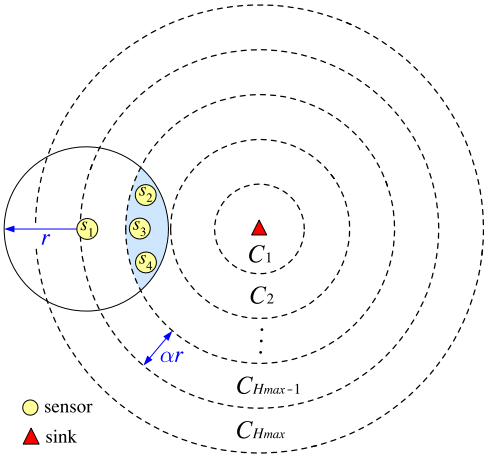

Fig. 5. Formation of corona structure. In this example, we set $\alpha = 4/7$.

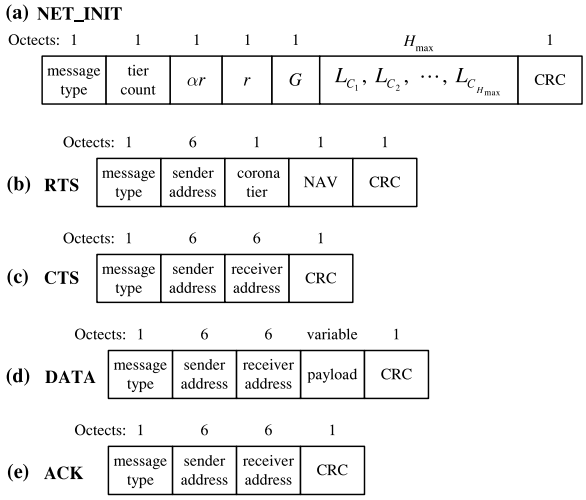

Fig. 6. Packet formats for Green-MAC.

anycast procedure, and a routing procedure. Before proceeding, we first present our protocol assumptions.

2.1 Assumptions

The assumptions behind the Green-MAC are listed as follows. (i) The sink is considered always awake. (ii) As in [6], [12], we assume that in the network area, sensors are randomly and uniformly deployed; besides, after the deployment, the positions of all sensors are static. (iii) As in [6], [12], we assume that sensors are time synchronized. According to [14], time synchronization can be easily accomplished in the WSN where sensors are equipped with GPS receivers [3]. For GPS-free WSNs, several industrial-strength time synchronization mechanisms have been proposed, including [7], [13], such that network-wide time synchronization error can be bounded within 255 μs [13], [30], which is less than one slot time [26]. Since employing CSMA/CA (carrier sense multiple access with collision avoidance) within a time frame, Green-MAC requires only coarse-grained time synchronization between each sensor and its next-hop group, and can tolerate such a small synchronization error. (See Section 2.4.) (iv) The transmission range of each sensor is adjustable between 0 and r meters. (v) We focus the WSN applications on event detection and reporting, where the sink is not required to communicate with a particular sensor, and the sensed event data is *always* destined for the sink [20].

2.2 Initial Configuration Procedure

The purpose of this procedure is to organize the WSN into equal-width coronas around the sink, as shown in Fig. 5. A by-product of this procedure is that the sink can flood the protocol parameters to all sensors. In Green-MAC, the protocol parameters include the transmission range αr of every sensor in the initial configuration phase, the transmission range r of every sensor after the initial configuration phase, the protocol constant G, and the cycle length L_{C_i} for the sensors in corona C_i, where $0 < \alpha < 1$, $1 \le i \le H_{\max}$, $H_{\max} = \left\lceil \frac{R}{\alpha r} \right\rceil$, and R is the radius of the region of the WSN. Note that we will present how to determine the appropriate values of L_{C_i} and α in Section 4.2 and Section 5.2, respectively. In order to create coronas, after the deployment of a WSN, the sink uses the power level corresponding to the transmission range αr to broadcast an NET_INIT packet with a field $tier\_count = 1$. Note that Fig. 6a depicts the packet format of NET_INIT. When a sensor receives an NET_INIT with $tier\_count = i$, the following process is triggered: If its $tier\_count$ has not been set or is larger than i, it stores the protocol parameters (i.e. $tier\_count$, G, and L_{C_i}), increases the value of $tier\_count$ field by one, and then rebroadcasts the NET_INIT packet with transmission range αr; otherwise, that NET_INIT will be discarded. After the initial configuration phase, the sensors with $tier\_count = i$ form the corona C_i, and the width of each corona is αr; moreover, each sensor in C_i thereafter fixes its transmission range and cycle length as r and L_{C_i}, respectively.

2.3 Wakeup/Sleep Schedule Scheme

For each sensor in Green-MAC, "the length of a cycle" and "the positions of ATFs/STFs in a cycle" must respectively adhere to the following rules:

- *Cycle length rule*. Given two integers $G \ge 1$ and $L_{\max} \ge 2G$, let $\mathcal{L} = \{G, G+1, \ldots, L_{\max}\}$. Let $\mathcal{L}_{\text{odd}} \subseteq \mathcal{L}$ and $\mathcal{L}_{\text{even}} \subseteq \mathcal{L}$ be the sets of *feasible* cycle lengths for the sensors in odd-tier coronas and even-tier coronas, respectively. Then for each $L \in \mathcal{L}_{\text{odd}}$ and $L' \in \mathcal{L}_{\text{even}}$, we require that the greatest common divisor of L and L', denoted by $\gcd(L, L')$, is no more than G.
- *Cycle pattern rule*. Assume that the cycle length of a sensor is L. Then for that sensor, in a cycle, the first consecutive G time frames are ATFs, while the residual $L - G$ time frames are STFs.

An example of $\mathcal{L}_{\text{odd}}$ and $\mathcal{L}_{\text{even}}$ is shown in Table 1, where we set $L_{\max} = 36$ and $G = 2$. Further, Fig. 7 illustrates, in Green-MAC, how two sensors, s_1 and s_2, in different but adjacent coronas arrange their individual ATFs. From Fig. 7, we can observe that two sensors, s_1 and s_2, can simultaneously wake up at the 10th reference time frame even if their schedule offset $\Delta(s_1, s_2) \ne 0$. Importantly, we have the following general result.

Theorem 1. *Green-MAC guarantees that in bounded time, any two sensors, say s_1 and s_2, in the neighboring coronas can*

TABLE 1
An Example of $\mathcal{L}_{\text{odd}}$ and $\mathcal{L}_{\text{even}}$

$\mathcal{L}_{\text{odd}}$	cycle length	2	4	5	7	10	14	19	23	29	
	ATF-ratio	1.000	0.500	0.400	0.286	0.200	0.143	0.105	0.087	0.069	
$\mathcal{L}_{\text{even}}$	cycle length	2	3	6	11	13	17	22	26	31	34
	ATF-ratio	1.000	0.667	0.333	0.181	0.153	0.118	0.091	0.077	0.065	0.059

wake up at the same time frame regardless of their schedule offset $\Delta(s_1, s_2)$ as well as their respective cycle lengths, L_{s_1} and L_{s_2}.

Proof. Without loss of generality, we assume that the schedule of s_1 leads that of s_2 by $\Delta(s_1, s_2) = t$ (in units of time frame). According to the cycle pattern rule, the set of the positions of ATFs in a cycle includes $\{0, 1, \ldots, G-1\}$. Thus from Fig. 7, we can observe that if one of s_1's ATFs and one of s_2's ATFs can mutually meet, there must exist some $x \in \{0, 1, \ldots, G-1\}$ and $y \in \{0, 1, \ldots, G-1\}$ such that the following system of congruences has infinitely many positive integer solutions z

$$\begin{cases} z \equiv x \pmod{L_{s_1}} \\ z \equiv t + y \pmod{L_{s_2}}, \end{cases} \tag{1}$$

where for positive integers a, b, and L, the notation "$a \equiv b \pmod{L}$" means that "$a \bmod L = b \bmod L$." Clearly, the solutions of z are the reference time frames at which both s_1 and s_2 simultaneously wake up. Take Fig. 7 for example. Given the schedule offset $\Delta(s_1, s_2) = 3$, s_1's 0th time frame (also an ATF) and s_2's 1st time frame (also an ATF) can meet each other at the 10th reference time frame since $10 \equiv 0 \pmod{10}$ and $10 \equiv 3 + 1 \pmod{6}$.

Since s_1 and s_2 are in the neighboring coronas, by cycle length rule, we have $\gcd(L_{s_1}, L_{s_2}) = g \leq G$. On the other hand, according to the *generalized Chinese remainder theorem* [9], equation (1) has infinitely many positive integer solutions if and only if $x \equiv t + y \pmod{g}$. Since the value of $(t + y) \bmod g$ falls in the set $\{0, 1, \ldots, g-1\}$, this theorem hence follows from the fact that $\{0, 1, \ldots, g-1\} \subseteq \{0, 1, \ldots, G-1\}$. □

2.4 Anycast and Routing Procedures

We assume that when a sensor detects an event, it should send its sensed data toward the sink. The routing procedure of Green-MAC works as follows. In Green-MAC, the sensors in corona C_i take responsibility for relaying the data sent from the sensors in corona C_{i+1} to the sensors in corona C_{i-1}. Since Green-MAC ensures that sensors in the neighboring coronas can simultaneously wake up in bounded time, a sensor with buffered event data, called *backlogged* sensor, can send its event packets to *any* one of the sensors in the inner adjacent corona. By this way, every sensor needs neither to broadcast beacons nor to maintain routing/neighbor tables, and the sensed data can be routed *corona-by-corona* from source sensors to the sink.

In what follows, we describe the anycast procedure of Green-MAC in detail. As illustrated in Fig. 8, when sensor s_1 intends to send event data destined for the sink, s_1 should first send an RTS (request-to-send) containing its *MAC address* and the *corona-tier* to ask for relaying. Each awake sensor in the next-hop group of s_1 that received the RTS should *backoff* to contend for sending a CTS (clear-to-send), where the *next-hop group* of a sensor s_1 in corona C_i is defined as the set of sensors in corona C_{i-1} that are in the transmission coverage of s_1. Taking Fig. 5 for example, sensors s_2, s_3, and s_4 together form the next-hop group of s_1. Upon receiving the CTS from s_2, s_1 sends a DATA to s_2, and s_2 then acknowledges its receipt. Note that if not receiving any CTS, s_1 may temporarily abort its anycast attempt and wait for the next time frame. The packet formats of RTS, CTS, DATA, and ACK in Green-MAC are shown in Fig. 6. In a dense WSN, the simultaneous contentions of RTSs and CTSs may easily result in collisions. Thus we employ our previously proposed *scalable backoff scheme* [27] to alleviate this problem. Specifically, before sending an RTS or a CTS, a sensor shall wait for an LIFS and a random backoff period $\text{SlotTime} \times B$, where LIFS stands for *long interframe space*, and B is a *reverse truncated geometric random variable* with parameter q, $0 < q < 1$. Importantly, we assign $\Pr(B = b) = (1-q)q^{CW-b}$ if $1 \leq b \leq CW$, and $\Pr(B = b) = q^{CW}$ if $b = 0$. According to [27], it can be shown that by scalable backoff scheme, the success probability of an RTS or a CTS can be nearly 90 percent even in a very dense WSN. Note that in our simulations, we set $q = 0.8$ and $CW = 31$.

To avoid the hidden terminal problem [19] and conserve energy, in an ATF, a sensor can immediately go to sleep whenever it hears an RTS, a CTS, or a DATA not intended for it, or the medium is sensed idle for a period of T_{listen}, where we set $T_{\text{listen}} = \text{LIFS} + CW + \max\{T_{\text{RTS}}, T_{\text{CTS}}\}$.

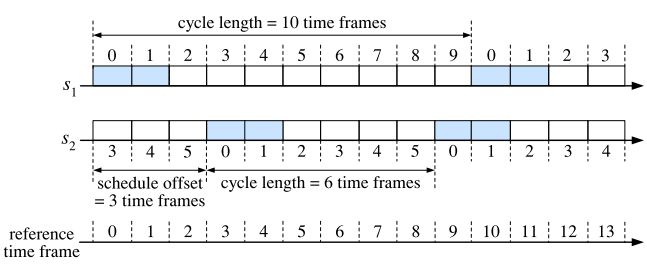

Fig. 7. An example of cycle patterns in Green-MAC, where we assume that $G = 2$.

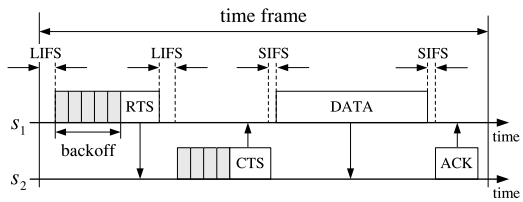

Fig. 8. An example of the anycast procedure in Green-MAC.

Normally, a backlogged sensor sends data only during its AFTs. However, to reduce anycast delay for time-sensitive applications, we could also adopt the *aggressive* anycast scheme, in which a backlogged sensor can keep trying to anycast data across multiple time frames (some of which may be originally STFs) until its buffered data is empty; thereafter, that sensor switches back to the normal wakeup/sleep mode.

3 Optimality of Green-MAC

In this section, we provide performance comparisons among Q-MAC [6], Queen-MAC [12], and Green-MAC with regard to the ATF-ratio and configurability.

Theorem 2. *In Green-MAC, given the protocol constant $G \geq 1$, the ATF-ratio of every sensor with a cycle length L is $G/L = O(1/L)$.*

Proof. Since G is a constant and independent of L, this theorem follows from the cycle pattern rule. □

Theorem 3. *Given the protocol constant $G \geq 1$ and the maximum cycle length $L_{\max} \geq 2G$, the number of configurable ATF-ratios $\theta(L_{\max})$ of each sensor in Green-MAC is in the order of $\Omega(L_{\max}/\ln L_{\max})$.*

Proof. Clearly, for a sensor in Green-MAC, the number of configurable ATF-ratios is equal to the number of feasible cycle lengths. Since the number of feasible cycle lengths for sensors in odd-tier coronas and even-tier coronas may be different, we define $\theta(L_{\max}) = \min\{|\mathcal{L}_{\text{odd}}|, |\mathcal{L}_{\text{even}}|\}$. To maximize the value of $\theta(L_{\max})$, we develop a simple and systematic method shown below to yield the feasible solutions of $\mathcal{L}_{\text{odd}}$ and $\mathcal{L}_{\text{even}}$ with the property $|\mathcal{L}_{\text{odd}}| \approx |\mathcal{L}_{\text{even}}|$.

- **S1.** Let $\mathcal{P} = \{p \mid p \text{ is a prime and } G \leq p \leq L_{\max}\}$. Let the truncated prime coset M_p be $\{p \times i \mid 1 \leq i \leq G \text{ and } p \times i \leq L_{\max}\}$. Let $\mathcal{U} = \bigcup_{p \in \mathcal{P}} M_p$.
- **S2.** *Evenly* partition $\mathcal{U}$ into two disjoint sets Q_1 and Q_2. Note that all members in M_p must be either in Q_1 or Q_2.
- **S3.** $\mathcal{L}_{\text{odd}} = \{G\} \cup Q_1$ and $\mathcal{L}_{\text{even}} = \{G\} \cup Q_2$.

For example, let $L_{\max} = 36$ and $G = 2$. Table 1 shows one possible solution of $\mathcal{L}_{\text{odd}}$ and $\mathcal{L}_{\text{even}}$, where $\mathcal{L}_{\text{odd}} = \{2\} \cup M_2 \cup M_5 \cup M_7 \cup M_{19} \cup M_{23} \cup M_{29}$ and $\mathcal{L}_{\text{even}} = \{2\} \cup M_3 \cup M_{11} \cup M_{13} \cup M_{17} \cup M_{31}$.

To calculate the value of $\theta(L_{\max})$, we first need to derive the cardinality of $\mathcal{U}$. Let $\pi(x)$ denote the number of primes not exceeding x. According to the prime number theorem [16], the value of $\pi(x)$ is at least $x \ln 2/(2 \ln x)$ for all real number $x \geq 2$, and equals to 0 otherwise. On the other hand, given $1 \leq k < G$ and $G \leq p \leq L_{\max}$, by **S1**, we have

$$|M_p| = \begin{cases} k, & \text{if } L_{\max}/(k+1) < p \leq L_{\max}/k, \\ G, & \text{if } G-1 < p \leq L_{\max}/G. \end{cases} \quad (2)$$

Let $num(M_{p \in \mathcal{P}}, k)$ be the number of different truncated prime cosets M_p, where $p \in \mathcal{P}$, whose cardinalities are all equal to k. Then we have

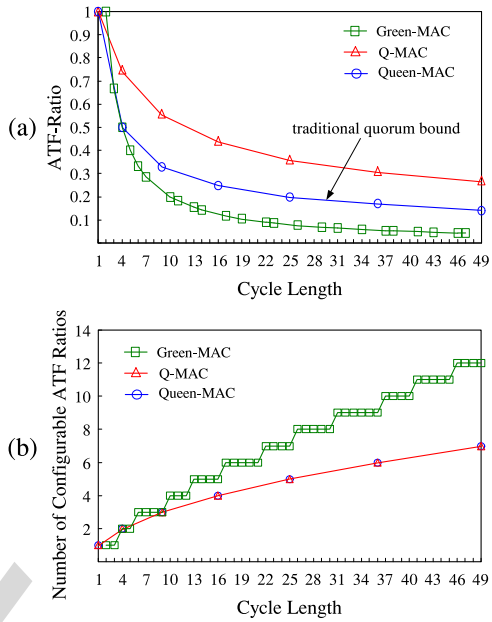

Fig. 9. Comparisons among Q-MAC, Queen-MAC, and Green-MAC. Here we set $G = 2$ and $L_{\max} = 49$. (a) The cycle length versus the ATF-ratio. (b) The cycle length versus the number of configurable ATF-ratios.

$$\begin{aligned} |\mathcal{U}| &= \sum_{k=1}^{G} k \times num(M_{p \in \mathcal{P}}, k) \\ &= \sum_{k=1}^{G-1} k\left[\pi\left(\frac{L_{\max}}{k}\right) - \pi\left(\frac{L_{\max}}{k+1}\right)\right] \\ &\quad + G\left[\pi(L_{\max}/G) - \pi(G-1)\right] \\ &= \sum_{k=1}^{G} \pi(L_{\max}/k) - G\pi(G-1) \\ &\geq \frac{\ln 2}{2} \sum_{k=1}^{G} \frac{(L_{\max}/k)}{\ln(L_{\max}/k)} - G\pi(G-1) \\ &\geq \frac{\ln 2}{2} \frac{L_{\max}}{\ln L_{\max}} \sum_{k=1}^{G} \frac{1}{k} - G\pi(G-1) \\ &\geq \frac{\ln 2}{2} \frac{L_{\max}}{\ln L_{\max}} \ln(G+1) - G\pi(G-1) \quad (3) \\ &= \Omega(L_{\max}/\ln L_{\max}). \quad (4) \end{aligned}$$

Note that inequality (3) follows by $\sum_{k=1}^{G}(1/k) \geq \int_{1}^{G+1}(1/x)dx = \ln(G+1)$ and equality (4) follows from the fact that both $\ln(G+1)$ and $G\pi(G-1)$ are constants since G is a constant. Finally, by **S2** and **S3**, we have $\theta(L_{\max}) = \min\{|\mathcal{L}_{\text{odd}}|, |\mathcal{L}_{\text{even}}|\} \geq \min\{|Q_1|, |Q_2|\} = \Omega(|\mathcal{U}|/2) = \Omega(L_{\max}/\ln L_{\max})$. □

Theorem 4. *The Green-MAC protocol is optimal and maximized configurable.*

Proof. It is a consequence of Theorems 2 and 3. □

Fig. 9 shows the theoretical performance comparisons among Q-MAC, Queen-MAC, and Green-MAC. We can find that Green-MAC outperforms Q-MAC and Queen-MAC in terms of both the ATF-ratio and configurability. To the best of our knowledge, Green-MAC is currently

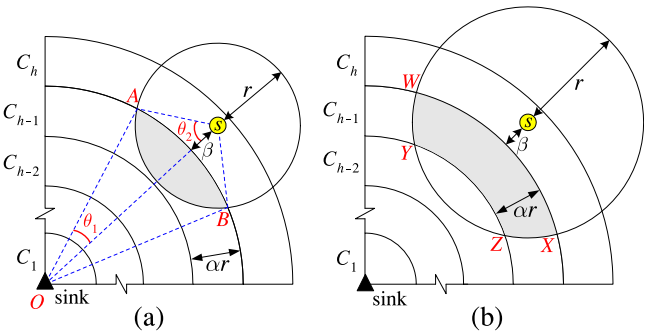

Fig. 10. The area of the shaded region (in each part) is denoted by $I_\beta(C_{h-1}, C_h)$. In part (a), the coverage of sensor s intersects with only C_{h-1}. In part (b), the coverage of sensor s intersects with both C_{h-1} and C_{h-2}.

the only known power saving protocol for a WSN where the ATF-ratio of *every* sensor with a cycle length L can be only $O(1/L)$, which breaks the traditional quorum bound $O(1/\sqrt{L})$.

4 Parameters Configuration and Performance Analysis

Fig. 9 demonstrates that one of the advantages of Green-MAC over Q-MAC and Queen-MAC is that it provides larger number of different feasible cycle lengths such that we can *more finely and precisely* configure the ATF-ratio of each sensor to achieve better performance. To illuminate this advantage, in this section, we show how to determine the proper cycle length of each sensor such that the average power consumption of a WSN is minimized while the worst event-to-sink delay constraint can be satisfied with high probability. To achieve this goal, we first need to derive the next-hop group size.

4.1 Next-Hop Group Size

Referring to Fig. 10, assume that there exists a sensor s in corona C_h, where $\lfloor 1/\alpha \rfloor + 1 \le h \le H_{\max}$. Let $I_\beta(C_{h-1}, C_h)$ be the area of the overlap between C_{h-1} and the transmission coverage of sensor s when the distance from s to the inner edge of corona C_h is β. Recall that the width of each corona is αr. This implies that $I_\beta(C_{h-1}, C_h) = 0$ when $\alpha \ge 1$ and $\beta = \alpha r$. Accordingly, we require α to be less than unity to ensure that every sensor has a chance to transfer data to its neighbors located in the adjacent inner corona. To calculate the value of $I_\beta(C_{h-1}, C_h)$, let us consider the following two cases.

Case 1. $\beta + \alpha r \ge r$, as shown in Fig. 10a. In this case, the transmission coverage of sensor s intersects with only C_{h-1}. Referring to Fig. 10a, let $R_{h-1} = (h-1)\alpha r$ be the distance from the sink to the outer edge of corona C_{h-1}; in addition, let $R_{h-1,\beta} = R_{h-1} + \beta$, $\angle AOs = \theta_1$, and $\angle AsO = \theta_2$. Then we have

$$\begin{aligned} I_\beta(C_{h-1}, C_h) &= area\_of\_lens(AB) \\ &= area\_of\_circular\_sector(OAB) \\ &\quad + area\_of\_circular\_sector(sAB) \\ &\quad - area\_of\_kite(sAOB) \\ &= \pi R_{h-1}^2 \frac{2\theta_1}{2\pi} + \pi r^2 \frac{2\theta_2}{2\pi} - R_{h-1} \sin\theta_1 \times R_{h-1,\beta}. \end{aligned} \tag{5}$$

Note that by the cosine rule for triangle $\triangle AOs$, we have $\theta_1 = \cos^{-1}\big((R_{h-1}^2 + R_{h-1,\beta}^2 - r^2)/2R_{h-1}R_{h-1,\beta}\big)$ and $\theta_2 = \cos^{-1}\big((r^2 + R_{h-1,\beta}^2 - R_{h-1}^2)/2rR_{h-1,\beta}\big)$.

Case 2. $\beta + \alpha r < r$, as shown in Fig. 10b. In this case, the transmission coverage of s intersects with both C_{h-1} and C_{h-2}. Similar to the derivation of equation (5), we have

$$\begin{aligned} &I_\beta(C_{h-1}, C_h) \\ &= area\_of\_lens(WX) - area\_of\_lens(YZ) \\ &= R_{h-1}^2 \cos^{-1}\left(\frac{R_{h-1}^2 + R_{h-1,\beta}^2 - r^2}{2R_{h-1}R_{h-1,\beta}}\right) \\ &\quad + r^2 \cos^{-1}\left(\frac{r^2 + R_{h-1,\beta}^2 - R_{h-1}^2}{2rR_{h-1,\beta}}\right) \\ &\quad - R_{h-1}R_{h-1,\beta} \sin\left(\cos^{-1}\left(\frac{R_{h-1}^2 + R_{h-1,\beta}^2 - r^2}{2R_{h-1}R_{h-1,\beta}}\right)\right) \\ &\quad - R_{h-2}^2 \cos^{-1}\left(\frac{R_{h-2}^2 + R_{h-1,\beta}^2 - r^2}{2R_{h-2}R_{h-1,\beta}}\right) \\ &\quad + R_{h-2}R_{h-1,\beta} \sin\left(\cos^{-1}\left(\frac{R_{h-2}^2 + R_{h-1,\beta}^2 - r^2}{2R_{h-2}R_{h-1,\beta}}\right)\right) \\ &\quad - r^2 \cos^{-1}\left(\frac{r^2 + R_{h-1,\beta}^2 - R_{h-2}^2}{2rR_{h-1,\beta}}\right). \end{aligned} \tag{6}$$

Assume that the sensor density is λ. The next-hop group size of sensor s is thus equal to $\lambda I_\beta(C_{h-1}, C_h)$. Now, we want to derive the minimum next-hop group area $I_{\min}(C_{h-1}, C_h)$, which will be used in deriving the proper cycle length for sensors in each corona. (See Section 4.2.) Clearly, the value of $I_\beta(C_{h-1}, C_h)$ is minimal when sensor s is at the outer edge of C_h (i.e. $\beta = \alpha r$). Let $h_0 = \lfloor 1/\alpha \rfloor$. The value of $I_{\alpha r}(C_{h-1}, C_h)$ can be further minimized with respect to h when h is made as small as possible, i.e., at $h_0 + 1$. This is because all sensors in C_i, for all $1 \le i \le h_0$, are within a distance r from the sink, and can thus transfer data directly to the sink. Let $K_{\min}$ be the minimum next-hop group size for any sensor in a WSN. Then we have $I_{\min}(C_{h-1}, C_h) = I_{\alpha r}(C_{h_0}, C_{h_0+1})$ and $K_{\min} = \lambda I_{\min}(C_{h-1}, C_h)$. Note that if we want a WSN to work well, we had better tune the values of α, r, and λ such that $K_{\min} \ge 1$. In Section 5.2, we will show how to determine the optimal value of α when the values of r and λ are given.

Next, we derive the average next-hop group area $I_{\text{avg}}(C_{h-1}, C_h)$, which will be used in evaluating the average power consumption of a WSN. (See Section 4.3.) The value of $I_{\text{avg}}(C_{h-1}, C_h)$ can be obtained by integrating the value of $I_\beta(C_{h-1}, C_h)$ and then dividing by the range of β. Let us consider the following two cases.

Case 1. $0 < \alpha < 0.5$, as illustrated in Fig. 10b. In this case, $\beta + \alpha r \le \alpha r + \alpha r < r$, which implies that the coverage of sensor s overlaps with more than one inner coronas. According to [21], (5) can be approximated by $\pi r(R_{h-1} + r - R_{h-1,\beta})/2$. According to (6), we have

$$\begin{aligned} I_\beta(C_{h-1}, C_h) &\approx \frac{\pi r(R_{h-1} + r - R_{h-1,\beta})}{2} \\ &\quad - \frac{\pi r(R_{h-2} + r - R_{h-1,\beta})}{2} = \frac{\pi r(R_{h-1} - R_{h-2})}{2} = \frac{\pi r^2 \alpha}{2}, \end{aligned} \tag{7}$$

which is independent of β. Therefore, we have $I_{\text{avg}}(C_h, C_{h-1}) \approx \pi r^2\alpha/2$.

Case 2. $0.5 \le \alpha < 1$. In this case, the coverage of sensor s may overlap with one or more inner coronas. For $0 < \beta < (1-\alpha)r$, the coverage of s overlaps with more than one inner coronas since $\beta + \alpha r < (1-\alpha)r + \alpha r = r$. For $(1-\alpha)r \le \beta \le \alpha r$, the coverage of s overlaps with only C_{h-1} since $\beta + \alpha r \ge (1-\alpha)r + \alpha r = r$. Thus we have

$$\begin{aligned} I_{\text{avg}}(C_h, C_{h-1}) &= \frac{1}{\alpha r}\int_0^{\alpha r} I_\beta(C_h, C_{h-1})d\beta \\ &\approx \frac{1}{\alpha r}\left(\int_0^{(1-\alpha)r} \frac{\pi r^2\alpha}{2}d\beta \right. \\ &\quad \left. + \int_{(1-\alpha)r}^{\alpha r} \frac{\pi r(R_{h-1} + r - R_{h-1,\beta})}{2}d\beta\right) \\ &= \frac{\pi r^2(4\alpha - 2\alpha^2 - 1)}{4\alpha}. \end{aligned} \tag{8}$$

Combining the results of the above two cases, the expected next-hop group size K_{avg} of a sensor in corona C_h can be expressed by (9) shown below

$$K_{\text{avg}} \approx \begin{cases} \frac{\lambda\pi r^2\alpha}{2} & \text{if } 0 < \alpha < 0.5, \\ \frac{\lambda\pi r^2(4\alpha - 2\alpha^2 - 1)}{4\alpha} & \text{if } 0.5 \le \alpha < 1. \end{cases} \tag{9}$$

It is worth noting that the approximate value of K_{avg} is dependent on α but independent of h, which implies that sensors located in different coronas have the same *expected* next-hop group size.

4.2 Configuration of Cycle Lengths

The configuration of cycle lengths essentially depends on the requirements of WSN applications. Recall that in this paper, we focus on the WSN application of event detection and reporting, in which the sensed event data has to be relayed to the sink *in time*. Thus we configure the cycle length of each sensor according to the following guidelines.

- **G1.** We think that all sensors in the same corona, say C_i, should have same cycle length since they equally share the responsibility of relaying event data from C_{i+1} to C_{i-1}.
- **G2.** We hope that sensors in different coronas have about the same lifetime since if all sensors in corona C_i die much earlier than those in other coronas, the event packets thereafter generated in C_j, for all $j > i$, will be unable to be relayed to the sink. Since we assume that events rarely occur, the ATF-ratio predominantly determines the lifetime of a sensor. Hence we require that $L_{C_i} \approx L_{C_j}$ for all $1 \le i \ne j \le H_{\max}$.
- **G3.** The value of L_{C_i} cannot be too large so as to ensure that the *worst* event-to-sink delay can be no more than T_{delay} (in units of time frame) with high probability $1 - \Phi$, where $0 \le \Phi < 1$ is a pre-specified real number.
- **G4.** Under the constraint of T_{delay}, the value of L_{C_i} should be as large as possible in order to minimize the power consumption of a WSN.

Let d_i denote the number of time frames required for a sensor in C_i to send a data packet to *any* one of its neighbors in C_{i-1}. According to **G3**, we need to configure the parameter L_{C_i}, for all $1 \le i \le H_{\max}$, such that the following inequality can be satisfied

$$\Pr\left(1 + \sum_{i=1}^{H_{\max}} d_i \le T_{\text{delay}}\right) \ge 1 - \Phi. \tag{10}$$

Note that the "1" in the left hand side of (10) reflects the fact that the source sensor begins to perform anycast *after* the time frame during which it detects an event. On the other hand, recall that every sensor in C_i, for all $1 \le i \le h_0$, can send a data packet *directly* to the sink within *one* time frame. Hence (10) is equivalent to (11) shown below

$$\Pr\left(2 + \sum_{i=h_0+1}^{H_{\max}} d_i \le T_{\text{delay}}\right) \ge 1 - \Phi. \tag{11}$$

Intuitively, the value of d_i increases as the next-hop group size of a backlogged sensor decreases. From Section 4.1, we know that the next-hop group size of any sensor is at least $K_{\min} = \lambda I_{\alpha r}(C_{h_0}, C_{h_0+1})$. Let $\mathcal{D}_{K_{\min}}(L)$ denote the anycast delay encountered by the sensor whose next-hop group size is $K_{\min}$ and the cycle lengths of whose next-hop group members are all equal to L. According to **G1** and **G2**, we hope that all sensors have about the same cycle length. If $L_{C_i} = L^*$ for all $1 \le i \le H_{\max}$, we can conclude that if (12) can be satisfied, so does (11)

$$\begin{aligned} &\Pr\left(2 + \sum_{i=h_0+1}^{H_{\max}} \mathcal{D}_{K_{\min}}(L^*) \le T_{\text{delay}}\right) \\ &= \Pr\left(\mathcal{D}_{K_{\min}}(L^*) \le \left\lfloor \frac{T_{\text{delay}} - 2}{H_{\max} - h_0} \right\rfloor\right) \ge 1 - \Phi. \end{aligned} \tag{12}$$

In what follows, we show the derivation of $\Pr(\mathcal{D}_{K_{\min}}(L) \le d)$ for given value of L and any positive integer d. We first assume that a sensor s has only one member s_i in its next-hop group whose cycle length is L. (Evidently, $\Pr(\mathcal{D}_{K_{\min}}(L) \le d) = 0$ if $K_{\min} = 0$. On the other hand, the next-hop group size of s may be larger than one; we will repair the current assumption in the next paragraph.) Recall that we can adopt the aggressive anycast scheme (stated in Section 2.4) to reduce the anycast delay. Let W_i be the random variable that represents the number of time frames from the reference time frame when s begins to anycast event data to s_i to the reference time frame when s_i wakes up. Since the schedule offset $\Delta(s, s_i)$ between s and s_i can be any integer between 0 and a sufficiently large number, according to cycle pattern rule, the probability mass function $f_{W_i}(d)$ and the cumulative distribution function $F_{W_i}(d)$ of W_i are respectively as follows:

$$f_{W_i}(d) = \Pr(W_i = d) = \begin{cases} G/L & \text{if } d = 1, \\ 1/L & \text{if } 2 \le d \le L - G + 1, \\ 0 & \text{otherwise.} \end{cases} \tag{13}$$

$$F_{W_i}(d) = \Pr(W_i \le d) = \begin{cases} (G+d-1)/L & \text{if } 1 \le d \le L-G+1, \\ 1 & \text{if } d > L-G+1. \end{cases} \quad (14)$$

Now, let us consider the case where the next-hop group size of sensor s is $K_{\min}$ and $K_{\min} \ge 1$. Let s_i be the ith member in the next-hop group of s. According to the aggressive anycast scheme, when s has data for the sink, the sensor[2] who wakes up *first* in the next-hop group of s will serve as the relaying sensor. Let $\mathcal{D}_{K_{\min}}(L) = \min_{1 \le i \le K_{\min}}\{W_i\}$. Clearly, $\mathcal{D}_{K_{\min}}(L)$ is the random variable that represents the anycast delay encountered by s. Since $W_1, \ldots, W_{K_{\min}}$ are independent and identical, we have $F_{W_i}(d) = F_{W_j}(d) = F(d)$, for all $1 \le i, j \le K_{\min}$, and

$$\begin{aligned} &\Pr\big(\mathcal{D}_{K_{\min}}(L) \le d\big) \\ &\quad = \Pr(\text{at least one of } W_i \text{ is no more than } d) \\ &\quad = \sum_{i=1}^{K_{\min}} \binom{K_{\min}}{i} (F(d))^i (1-F(d))^{K_{\min}-i}. \end{aligned} \quad (15)$$

To meet **G4** and satisfy inequality (12), we can let

$$L^* = \max\Big\{ L \;\Big|\; \Pr\Big(\mathcal{D}_{K_{\min}}(L) \le \Big\lfloor \frac{T_{\text{delay}} - 2}{H_{\max} - h_0} \Big\rfloor\Big) \ge 1 - \Phi \text{ and } G \le L \le L_{\max} \Big\}. \quad (16)$$

However, L^* may not be the feasible cycle length for every sensor in a WSN. Let L_{odd} and L_{even} be the cycle lengths for the sensors in odd-tier coronas and even-tier coronas, respectively. To meet **G1**, **G2**, **G3**, and **G4**, we set $L_{\text{odd}} = \max\{L \mid L \le L^* \text{ and } L \in \mathcal{L}_{\text{odd}}\}$ and $L_{\text{even}} = \max\{L \mid L \le L^* \text{ and } L \in \mathcal{L}_{\text{even}}\}$.

4.3 Average Power Consumption of a WSN

The power consumption P_{WSN} of a WSN running GreenMAC consists of two components. First, even though there is no traffic, all sensors still need to consume power P_{PS} to run the power-saving mode whereby each sensor sleeps, wakes up, remains awake for a certain time T_{listen}, then sleeps again, and so forth according to the cycle pattern rule. Second, once an event of interest is detected, the sensors along the path from source to the sink together consume power P_{report} to relay the data of event report. Thus we have $\mathbb{E}[P_{\text{WSN}}] = \mathbb{E}[P_{\text{PS}}] + \mathbb{E}[P_{\text{report}}]$, where $\mathbb{E}[\cdot]$ denotes the expectation value.

We first show the derivation of $\mathbb{E}[P_{\text{PS}}]$. Let F denote the length of a time frame. Let N_{odd} and N_{even} denote the total number of sensors in odd-tier coronas and even-tier coronas, respectively. Since there are G ATFs in a cycle, and each sensor goes to sleep in an ATF when the channel is sensed idle for T_{listen}, we have

$$\begin{aligned} &\mathbb{E}[P_{\text{PS}}] \\ &= N_{\text{odd}} \Big[\frac{G\big(E_{\text{switch}} + P_{\text{on}} T_{\text{listen}} + P_{\text{off}}(F - T_{\text{listen}})\big) + P_{\text{off}}(L_{\text{odd}} - G)F}{L_{\text{odd}} F} \Big] \\ &+ N_{\text{even}} \Big[\frac{G\big(E_{\text{switch}} + P_{\text{on}} T_{\text{listen}} + P_{\text{off}}(F - T_{\text{listen}})\big) + P_{\text{off}}(L_{\text{even}} - G)F}{L_{\text{even}} F} \Big], \end{aligned}$$

where E_{switch} is the energy consumption on the transition between sleep state and awake state, P_{on} and P_{off} are the power consumptions when the radio module is on and off, respectively. Since the area of the corona C_i is $(2i-1)\pi(\alpha r)^2$ for all $1 \le i \le H_{\max} - 1$, we have

$$N_{\text{odd}} = \begin{cases} \frac{H_{\max}}{2}(H_{\max}-1)\lambda\pi(\alpha r)^2 & \text{if } H_{\max} \text{ is even,} \\ \lambda\pi R^2 - \lfloor \frac{H_{\max}}{2} \rfloor \big(2\lfloor \frac{H_{\max}}{2} \rfloor + 1\big)\lambda\pi(\alpha r)^2 & \text{if } H_{\max} \text{ is odd} \end{cases} \quad (17)$$

and $N_{\text{even}} = \lambda\pi R^2 - N_{\text{odd}}$.

Next, we show the derivation of $\mathbb{E}[P_{\text{report}}]$. Assume that in a WSN, the average inter-event time is $T_{\text{event}}^{\text{WSN}}$. Let H_{avg} be the expected *tier* number of the corona where an event occurs. Let $E_{\text{report}}(C_h)$ denote the average total energy required to send the report of an event from a sensor in C_h to the sink. Then we have $\mathbb{E}[P_{\text{report}}] = E_{\text{report}}(C_{\lceil H_{\text{avg}} \rceil})/T_{\text{event}}^{\text{WSN}}$. Note that since an event is equally likely to occur at any sensor in the region, the probability of an event occurring in C_i is $(2i-1)(\alpha r/R)^2$, and we have

$$\begin{aligned} H_{\text{avg}} = &\sum_{i=1}^{H_{\max}-1} i(2i-1)\Big(\frac{\alpha r}{R}\Big)^2 \\ &+ H_{\max}\Big[1 - (H_{\max}-1)^2\Big(\frac{\alpha r}{R}\Big)^2\Big]. \end{aligned} \quad (18)$$

In what follows, we show the derivation of $E_{\text{report}}(C_h)$. Assume that an event $\mathcal{V}$ is detected by a sensor s_h, and relayed by sensors $s_{h-1}, s_{h-2}, \ldots, s_{h_0}$ to the sink, where $s_i \in C_i$ and $h_0 \le i \le h$. For the convenience of notation, we denote by s_{h_0-1} the sink, and assume that the cycle length of the sink, denoted by $L_{C_{h_0-1}}$, is G to reflect the fact that the sink is always awake. The value of $E_{\text{report}}(C_h)$ can be broken up into the following four components.

Component 1. *The energy consumed by the sensors on the path $s_h \rightsquigarrow s_{h_0}$ to wake up in their STFs.* Let $\mathcal{S}_{\text{path}}(C_h)$ denote the average total number of awake-STFs of the sensors on the path $s_h \rightsquigarrow s_{h_0}$. Then we have

$$E_{\text{component1}} = \big[(P_{\text{on}} - P_{\text{off}})T_{\text{listen}} + E_{\text{switch}}\big]\mathcal{S}_{\text{path}}(C_h). \quad (19)$$

Further, the value of $\mathcal{S}_{\text{path}}(C_h)$ can be broken up into the following two parts.

Part 1. *The average number of awake-STFs of s_h, $\mathcal{S}_{\text{source}}(C_h)$.* Let $\mathcal{A}(f, d)$ be the number of ATFs *after* the time frame f in which s_h detects $\mathcal{V}$ to the time frame in which s_h successfully sends that event data to s_{h-1}, under the condition that the anycast delay from s_h to s_{h-1} is d. Take Fig. 11a for example. Assume that s_h detects event $\mathcal{V}$ in the sixth time frame, and then keeps trying to anycast that event data to s_{h-1} from the seventh time frame. In such an example, the anycast delay d is 5, $\mathcal{A}(6, 5) = 3$, and the number of STFs

2. If multiple next-hop neighbors of s wake up in the same time frame, the sensor who replies CTS first will serve as the relaying sensor. To simplify the analysis, we assume that no collisions occur during the RTS/CTS handshakes. Definitely, we will remove this assumption in simulations. See Sections 5.2 and 5.4.

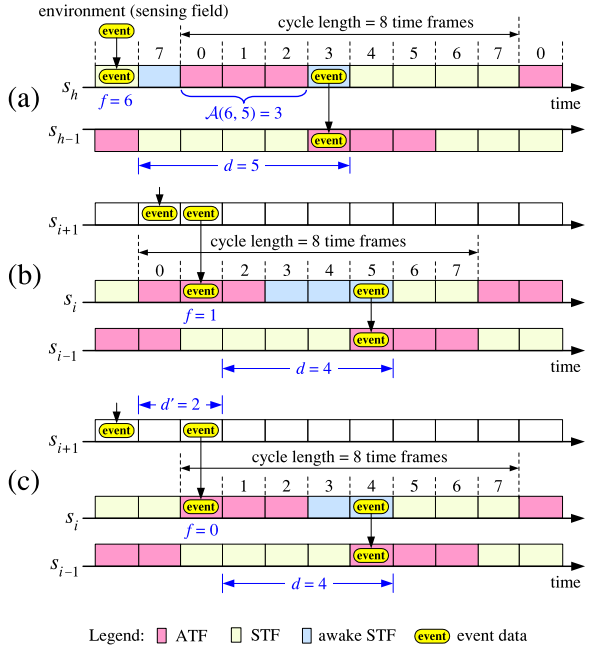

Fig. 11. The relationship between anycast delay and the number of awake-STFs. In part (a), we assume that $G = 3$, $L_{C_h} = 8$, and $L_{C_{h-1}} = 7$. In parts (b) and (c), we assume that $G = 3$, $L_{C_i} = 8$, and $L_{C_{i-1}} = 7$.

during which s_h needs to wake up is $d - \mathcal{A}(f,d) = 5 - 3 = 2$. Recall that according to (13), the value of d is no more than $L_{C_{h-1}} - G + 1$. Since event $\mathcal{V}$ may occur in any time frame in a cycle, we have

$$\begin{aligned}\mathcal{S}_{\text{source}}(C_h) &= \sum_{f=0}^{L_{C_h}-1}\left\{\frac{1}{L_{C_h}}\sum_{d=1}^{L_{C_{h-1}}-G+1}\right.\\ &\quad\left.\Pr\big(\mathcal{D}_{K_{\text{avg}}}(L_{C_{h-1}}) = d\big) \times \big[d - \mathcal{A}(f,d)\big]\right\}\\ &= \sum_{d=1}^{L_{C_{h-1}}-G+1}\Pr\big(\mathcal{D}_{K_{\text{avg}}}(L_{C_{h-1}}) = d\big) \times d\\ &\quad - \frac{1}{L_{C_h}}\sum_{f=0}^{L_{C_h}-1}\sum_{d=1}^{L_{C_{h-1}}-G+1}\\ &\quad \Pr\big(\mathcal{D}_{K_{\text{avg}}}(L_{C_{h-1}}) = d\big) \times \mathcal{A}(f,d).\end{aligned} \tag{20}$$

Note that according to (9), sensors located in any coronas have the same expected next-hop group size K_{avg}; according to (15), we have $\Pr\big(\mathcal{D}_{K_{\text{avg}}}(L) = d\big) = \Pr\big(\mathcal{D}_{K_{\text{avg}}}(L) \le d\big) - \Pr\big(\mathcal{D}_{K_{\text{avg}}}(L) \le d-1\big)$.

To derive the second term in the right hand side of (20), we first swap the indices f and d in the double summation. In other words, we have

$$\begin{aligned}&\sum_{f=0}^{L_{C_h}-1}\sum_{d=1}^{L_{C_{h-1}}-G+1}\Pr\big(\mathcal{D}_{K_{\text{avg}}}(L_{C_{h-1}}) = d\big) \times \mathcal{A}(f,d)\\ &= \sum_{d=1}^{L_{C_{h-1}}-G+1}\sum_{f=0}^{L_{C_h}-1}\Pr\big(\mathcal{D}_{K_{\text{avg}}}(L_{C_{h-1}}) = d\big) \times \mathcal{A}(f,d).\end{aligned} \tag{21}$$

To derive the approximate value of the right hand side of (21), we ignore the cases where $d > L_{C_h} - G + 1$ if $L_{C_{h-1}} > L_{C_h}$. Such a simplification is justifiable since we demand $L_{C_h} \approx L_{C_{h-1}}$; under such circumstances, the value of $\Pr(\mathcal{D}_{K_{\text{avg}}}(L_{C_{h-1}}) > L_{C_h} - G + 1 \,|\, L_{C_{h-1}} \gtrsim L_{C_h})$ is negligible. For example, if $L_{C_{h-1}} = 31$, $L_{C_h} = 29$, $G = 2$, and $K_{\text{avg}} = 7$, then $\Pr(\mathcal{D}_7(31) > 28) = 4.65 \times 10^{-9}$. Importantly, we make the following observations: Given that $1 \le d \le G$, if we fix the value of d and then increase the value of f one by one from 0 to $L_{C_h} - 1$, the value of $\mathcal{A}(f,d)$ will sequentially become

$$\begin{aligned}&\underbrace{d, d, \ldots, d}_{(G-d+1)\text{times}}, d-1, d-2, \ldots, 2, 1,\\ &\underbrace{0, 0, \ldots, 0,}_{(L_{C_h}-G-d+1)\text{times}} \quad 1, 2, \ldots, d-2, d-1.\end{aligned} \tag{22}$$

On the other hand, given that $G < d \le L_{C_{h-1}} - G + 1$, if we fix the value of d and then increase the value of f one by one from 0 to $L_{C_h} - 1$, the value of $\mathcal{A}(f,d)$ will sequentially become

$$\begin{aligned}&G, G-1, \ldots, 2, 1, \quad \underbrace{0, 0, \ldots, 0,}_{(L_{C_h}-G-d+1)\text{times}}\\ &1, 2, \ldots, G-1, G, \underbrace{G, G, \ldots, G}_{(d-G-1)\text{times}}.\end{aligned} \tag{23}$$

Accordingly, we have

$$\begin{aligned}&\sum_{d=1}^{L_{C_{h-1}}-G+1}\sum_{f=0}^{L_{C_h}-1}\Pr\big(\mathcal{D}_{K_{\text{avg}}}(L_{C_{h-1}}) = d\big)\\ &\quad\times\ \mathcal{A}(f,d) \approx \sum_{d=1}^{G}\left\{\Pr\big(\mathcal{D}_{K_{\text{avg}}}(L_{C_{h-1}}) = d\big)\right.\\ &\quad\left.\times\left[d(G-d+1) + 2\sum_{i=1}^{d-1} i\right]\right\}\\ &\quad+ \sum_{d=G+1}^{L_{C_{h-1}}-G+1}\left\{\Pr\big(\mathcal{D}_{K_{\text{avg}}}(L_{C_{h-1}}) = d\big)\right.\\ &\quad\left.\times\left[G(d-G-1) + 2\sum_{i=1}^{G} i\right]\right\}\\ &= \sum_{d=1}^{G}\Pr\big(\mathcal{D}_{K_{\text{avg}}}(L_{C_{h-1}}) = d\big) \times dG\\ &\quad+ \sum_{d=G+1}^{L_{C_{h-1}}-G+1}\Pr\big(\mathcal{D}_{K_{\text{avg}}}(L_{C_{h-1}}) = d\big) \times Gd\\ &= G\sum_{d=1}^{L_{C_{h-1}}-G+1}\Pr\big(\mathcal{D}_{K_{\text{avg}}}(L_{C_{h-1}}) = d\big) \times d.\end{aligned} \tag{24}$$

Part 2. *The average number of awake-STFs of s_i, $\mathcal{S}_{\text{relay}}(C_i)$, for all $h_0 \le i \le h-1$.* Since s_i takes responsibility for relaying the event data from s_{i+1} to s_{i-1}, let us consider the following two conditions.

Condition 1. *The number of time frames required by s_{i+1} to send the event data to s_i is exactly* 1, which implies that s_i is currently in an ATF when s_{i+1} tries to relay the event data to s_i. Let, under Condition 1, $S_{\text{relay}}^{\text{cond\_1}}(C_i)$ denote the random variable that represents the number of awake-STFs of s_i when s_i tries to send that event data to s_{i-1}. Assume that s_i

receives the event data from s_{i+1} in its fth time frame. As illustrated in Fig. 11b, $S_{\text{relay}}^{\text{cond\_1}}(C_i)$ will be 0 if the number of time frames d required by s_i to send that event data to s_{i-1} is no more than $G-f-1$; otherwise, $S_{\text{relay}}^{\text{cond\_1}}(C_i)$ will be $d-G+f+1$. Since under Condition 1, s_i can be currently in arbitrary one of its ATFs, we have

$$\begin{aligned}\mathbb{E}\big[S_{\text{relay}}^{\text{cond\_1}}(C_i)\big] &= \sum_{f=0}^{G-1}\left[\frac{1}{G}\sum_{d=1}^{L_{C_{i-1}}-G+1}\Pr\big(\mathcal{D}_{K_{\text{avg}}}(L_{C_{i-1}})=d\big)\times S_{\text{relay}}^{\text{cond\_1}}(C_i)\right]\\ &= \frac{1}{G}\sum_{f=0}^{G-1}\sum_{d=G-f}^{L_{C_{i-1}}-G+1}\Pr\big(\mathcal{D}_{K_{\text{avg}}}(L_{C_{i-1}})=d\big)\times(d-G+f+1).\end{aligned} \tag{25}$$

Condition 2: *The number of time frames d' required by s_{i+1} to send the event data to s_i is larger than* 1, as shown in Fig. 11c where $d'=2$, which implies that s_i is currently in an STF when s_{i+1} tries to relay the event data to s_i. Under such circumstances, s_{i-1} will receive that even data in its *zeroth* time frame (which is also an ATF). Let $S_{\text{relay}}^{\text{cond\_2}}(C_i)$ denote the random variable that represents the number of awake-STFs of s_i when s_i tries to send that event data to s_{i-1}. Assume that s_i receives the event data from s_{i+1} in its fth time frame. As illustrated in Fig. 11c, $S_{\text{relay}}^{\text{cond\_2}}(C_i)$ will be 0 if the number of time frames d required by s_i to send that event data to s_{i-1} is no more than $G-1$; otherwise, $S_{\text{relay}}^{\text{cond\_2}}(C_i)$ will be $d-G+1$. Thus we have

$$\begin{aligned}\mathbb{E}\big[S_{\text{relay}}^{\text{cond\_2}}(C_i)\big] &= \sum_{d=1}^{L_{C_{i-1}}-G+1}\Pr\big(\mathcal{D}_{K_{\text{avg}}}(L_{C_{i-1}})=d\big)\times S_{\text{relay}}^{\text{cond\_2}}(C_i)\\ &= \sum_{d=G}^{L_{C_{i-1}}-G+1}\Pr\big(\mathcal{D}_{K_{\text{avg}}}(L_{C_{i-1}})=d\big)\times\ (d-G+1).\end{aligned} \tag{26}$$

Let $\mathcal{S}_{\text{relay}}(C_i)$ be the average number of awake-STFs of s_i for all $h_0 \le i \le h-1$. By jointly considering Condition 1 and Condition 2, we have

$$\begin{aligned}\mathcal{S}_{\text{relay}}(C_i) = \Pr\big(\mathcal{D}_{K_{\text{avg}}}(L_i)=1\big)\times\mathbb{E}\big[S_{\text{relay}}^{\text{cond\_1}}(C_i)\big]\\ +\big[1-\Pr\big(\mathcal{D}_{K_{\text{avg}}}(L_i)=1\big)\big]\times\mathbb{E}\big[S_{\text{relay}}^{\text{cond\_2}}(C_i)\big].\end{aligned} \tag{27}$$

Then combining the derivations of Part 1 and Part 2 leads to the following result:

$$\mathcal{S}_{\text{path}}(C_h)=\begin{cases}\mathcal{S}_{\text{source}}(C_h) & \text{if } h\le h_0,\\ \mathcal{S}_{\text{source}}(C_h)+\sum_{i=h_0}^{h-1}\mathcal{S}_{\text{relay}}(C_i) & \text{if } h>h_0.\end{cases} \tag{28}$$

Component 2. *The energy consumed by sensor s_i to send futile RTSs to s_{i-1} for all $h_0+1\le i\le h$*. Clearly, if the anycast delay from s_i to s_{i-1} is $\mathcal{D}(L_{C_{i-1}})$, there will be $\mathcal{D}(L_{C_{i-1}})-1$ futile RTSs. Let P_{tx} denote the power consumed by the wireless network interface in transmitting state. We have

$$\begin{aligned}E_{\text{component2}} = \sum_{i=h_0+1}^{h}(P_{\text{tx}}-P_{\text{on}})\\ \times\sum_{d=1}^{L_{C_{i-1}}-G+1}\Pr\big(\mathcal{D}_{K_{\text{avg}}}(L_{C_{i-1}})=d\big)\times(d-1)T_{\text{RTS}}.\end{aligned} \tag{29}$$

Component 3. *The energy consumed by the sensors on the path $s_h \rightsquigarrow s_{h_0}$ to stay awake for executing the task of relaying the event data*. Note that the total number of time frames required by s_h to execute the task is *one* since it needs only to forward the data to s_{h-1}, while the total number of time frames required by s_i, for all $h_0\le i\le h-1$, to execute the task is *two*: one for receiving the data from s_{i+1} and one for forwarding the data to s_{i-1}, where we assume that s_{h_0-1} is the sink. Hence we have

$$\begin{aligned}E_{\text{component3}} = (P_{\text{on}}-P_{\text{off}})(F-T_{\text{listen}})\\ +\sum_{i=h_0}^{h-1}2(P_{\text{on}}-P_{\text{off}})(F-T_{\text{listen}}).\end{aligned} \tag{30}$$

Component 4. *The energy consumed by the sensors on the path $s_h \rightsquigarrow s_{h_0}$ to perform the four-way handshakes, i.e. RTS/CTS/DATA/ACK*. Specifically, sensor s_i, for all $h_0\le i\le h$, needs to transmit an RTS and a DATA to s_{i-1} as well as to receive a CTS and an ACK from s_{i-1}, where we assume that s_{h_0-1} is the sink. On the other hand, sensor s_i, for all $h_0\le i\le h-1$, needs to transmit a CTS and an ACK to s_{i+1} as well as to receive an RTS and a DATA from s_{i+1}. Note that we do not count the energy consumption of the sink, which is often considered to have unlimited power supply. Let P_{rx} denote the power consumed by the wireless network interface in receiving state. Then we have

$$\begin{aligned}E_{\text{component4}} = \sum_{i=h_0}^{h}\big[(P_{\text{tx}}-P_{\text{on}})(T_{\text{RTS}}+T_{\text{DATA}})\\ +(P_{\text{rx}}-P_{\text{on}})(T_{\text{CTS}}+T_{\text{ACK}})\big]\\ +\sum_{i=h_0}^{h-1}\big[(P_{\text{tx}}-P_{\text{on}})(T_{\text{CTS}}+T_{\text{ACK}})\\ +(P_{\text{rx}}-P_{\text{on}})(T_{\text{RTS}}+T_{\text{DATA}})\big].\end{aligned} \tag{31}$$

Finally, by combining the results of (19), (29), (30), and (31), we have

$$\begin{aligned}E_{\text{report}}(C_h) = E_{\text{component1}}+E_{\text{component2}}\\ +\ E_{\text{component3}}+E_{\text{component4}}.\end{aligned} \tag{32}$$

5 Performance Evaluation

5.1 Simulation Model

We follow the event-driven approach [22] (which has been adopted and validated in our previous studies [8, page. 4]) to build the simulators to compare the performances of Green-MAC to those of Q-MAC [6] and Queen-MAC [12]. In our simulations, sensors are initially randomly and uniformly placed in a circular region of radius 250 m, centered at the sink. After the initial configuration phase, the transmission range r of each sensor is fixed at 75 m. Besides, we assume that each sensor generates an event packet with 128 bytes every $T_{\text{event}}^{\text{sensor}}$ seconds, where $T_{\text{event}}^{\text{sensor}} \gg F$. Note that when there are N sensors in a WSN, we have $T_{\text{event}}^{\text{WSN}} = T_{\text{event}}^{\text{sensor}}/N$. In Green-MAC, we set $G=2$ and demand that the worst event-to-sink delay requirement must be fulfilled with probability at least 90 percent, i.e. $\Phi = 0.1$. Table 2 summarizes the system parameter values, which mainly follow the

TABLE 2
System Parameters Used in Simulations

Parameter	Value
Channel bit rate	250 Kbps
Time frame length	30 ms
LIFS	640 μs
SIFS	192 μs
SlotTime	320 μs
Contention window	31 slots
Maximum idle sensing time (T_{listen})	11 ms
Power consumption in TRANSMIT state	52.2 mW
Power consumption in RECEIVE state	56.4 mW
Power consumption in LISTEN state	56.4 mW
Power consumption in SLEEP state	0.06 μW
Energy consumption of SLEEP/AWAKE transition	0.83 μJ

specifications adopted in [17] and the datasheet of CC2420 [26] by Texas Instruments. Note that since we assume that sensors are static, the channel quality is relatively stable [19], the throughput loss due to link errors is only about 1 percent [26], [29] and can be thus negligible.

Now, we briefly describe how sensors in Q-MAC and Queen-MAC configure their respective ATF-ratios according to the traffic load [6], [12]. In Q-MAC and Queen-MAC, $\alpha = 1$. Let $H^Q_{\max} = \lceil R/r \rceil$ and $area_Q(C_i)$ denote the area of the corona C_i in Q-MAC and Queen-MAC. Then $area_Q(C_i)$ equals to $(2i-1)\pi r^2$ for $1 \le i \le H^Q_{\max} - 1$, and $\pi[R^2 - (H^Q_{\max} - 1)^2 r^2]$ if $i = H^Q_{\max}$. Let $traffic(C_i)$ denote the traffic load (i.e. the average number of event packets that must be *handled* per second) of each sensor in corona C_i. According to [6], the sensors in C_i need to help the sensors in C_{i+1} to relay event packets to the sink. Therefore,

$$traffic(C_i) = \begin{cases} T^{\text{sensor}}_{\text{event}} & \text{if } i = H^Q_{\max}, \\ \frac{1}{T^{\text{sensor}}_{\text{event}}} + \frac{area_Q(C_{i+1})}{area_Q(C_i)} \times traffic(C_{i+1}) & \text{if } 1 \le i \le H^Q_{\max} - 1. \end{cases} \quad (33)$$

From Section 1.1, we know that if the cycle length of a sensor in Q-MAC is L, then for that sensor, the average number of ATFs per second is $(2\sqrt{L} - 1)/(L \times F)$. Thus in Q-MAC, the cycle length $L^{\text{Q}}_{C_i}$ of a sensor in C_i is configured by (34)

$$L^{\text{Q}}_{C_i} = \max\{L \mid \sqrt{L} \ge 1 \text{ is an integer and } (2\sqrt{L} - 1)/(L \times F) \ge traffic(C_i)\}. \quad (34)$$

In Queen-MAC, all sensors have the same cycle length L^{Queen}, and the consecutive L^{Queen} time frames are arranged as a $\sqrt{L^{\text{Queen}}} \times \sqrt{L^{\text{Queen}}}$ grid in a row-major fashion; moreover, a sensor in the outermost corona can select only *one* row (or column) from the grid as its ATFs. Thus Queen-MAC requires that $traffic(C_{H^Q_{\max}}) = 1/T^{\text{sensor}}_{\text{event}} \le \sqrt{L^{\text{Queen}}}/(L^{\text{Queen}} \times F)$. This implies that the cycle length L^{Queen} of every sensor in Queen-MAC can be configured as (35)

$$L^{\text{Queen}} = \max\{L \mid \sqrt{L} \ge 1 \text{ is an integer and } L \le (T^{\text{sensor}}_{\text{event}}/F)^2\}. \quad (35)$$

Assume that in Queen-MAC, a sensor in C_i selects k_i rows (or columns) from the $\sqrt{L^{\text{Queen}}} \times \sqrt{L^{\text{Queen}}}$ grid as its ATFs. This implies that for a sensor in C_i, the average number of ATFs per second is $(k_i \times \sqrt{L^{\text{Queen}}})/(L^{\text{Queen}} \times F)$. On the other hand, a sensor can either transmit or receive only one data packet in a time frame. This implies that a sensor requires two time frames to relay one event packet. Accordingly, Queen-MAC demands that

$$k_i = \min\left\{ k \;\middle|\; k \in \mathbb{Z}^+ \text{and} \frac{k \times \sqrt{L^{\text{Queen}}}}{L^{\text{Queen}} \times F} \ge 2 \times traffic(C_i) - (1/T^{\text{sensor}}_{\text{event}}) \right\}. \quad (36)$$

Four major metrics are used in our performance evaluation: delay violation ratio, event-to-sink throughput, network lifetime, and survival ratio. The *delay violation ratio* is defined as the fraction of event packets that did not reach the sink within the delay requirement T_{delay}. The *event-to-sink throughput* is defined by dividing the amount of event data traveling from sources to the sink within the delay constraint by the entire simulation time. The *network lifetime* is defined as the time until all observed sensors are dead due to energy exhaustion. The *survival ratio* is defined as the number of surviving observed sensors (with nonzero energy) over the total number of observed sensors. Note that when measuring the network lifetime and survival ratio, we assume that the initial energy of each sensor is 5 J and observe merely the sensors whose distances to the sink are no more than r. Such an experimental arrangement is justifiable since if all observed sensors are dead, other alive sensors are unable to forward event data to the sink. Note that in the following graphs, the values of $K_{\min}$ (i.e. minimum next-hop group size) are all from simulation results (i.e. the nearest integer of the average minimum next-hop group size); besides, the ideal cycle length (L^*) of each sensor is derived by equations (15) and (16), where the value of $K_{\min}$ is adopted from simulation results to faithfully reflect the simulated environments.

5.2 Effect of α

The purpose of this section is to verify our theoretical analysis (presented in Section 4). From Sections 2.1 and 4.1, we know that in Green-MAC, $0 < \alpha < 1$. Thus in the experiments of Fig. 12, we vary the value of α from 0.15 to 0.85. Besides, we assume that (i) $T^{\text{sensor}}_{\text{event}} = 20$, (ii) the total number of sensors is 500, and (iii) the event-to-sink delay requirement is 2 s. From Fig. 12a, we can see that for each α, the difference between the value of $K_{\min}$ derived from analysis results and that obtained from simulation results is small. Above all, Fig. 12a shows that as the value of α increases, the value of $H_{\max}$ (i.e. maximum hops from source to sink) decreases, while the value of $K_{\min}$ initially increases and then begins to drop when $\alpha \ge 0.5$. The reasons are as follows. In Green-MAC, the transmission range of a sensor is fixed at r after the initial configuration phase. Therefore, as the value of α increases, the corona width (αr) becomes wider, and the total number of coronas decreases, causing the value of $H_{\max}$ to become smaller. On the other hand, when the value of α begins to increase, the overlapping area

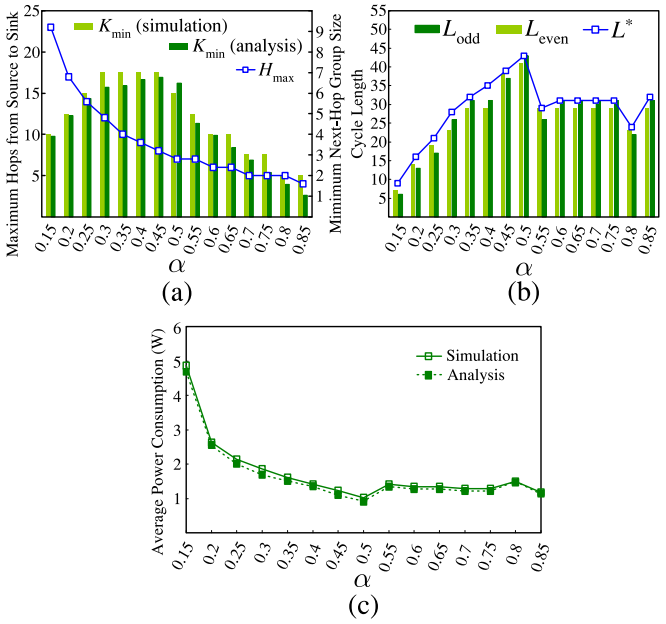

Fig. 12. (a) α versus "maximum hops from source to sink" and "minimum next-hop group size." (b) α versus cycle length (in units of time frames). (c) α versus average power consumption of a WSN.

of C_{i-1} and the transmission coverage of a sensor in C_i increases as well; however, when $\alpha \geq 0.5$, this overlapping area begins to shrink since the transmission range of a sensor at the outer edge of C_i is now unable to reach the inner edge of C_{i-1}.

Fig. 12b shows the ideal cycle length (L^*) of each sensor. We can find that as the value of α increases, the value of L^* initially increases and then begins to decrease with some moderate oscillations when $\alpha > 0.5$. From Sections 4.1 and 4.2, we can understand that the value of L^* depends on $H_{\max}$ and $K_{\min}$, both of which further depend on α. Although when the value of α rises from 0.5, the value of $H_{\max}$ declines, yet the value of $K_{\min}$ declines as well. Fig. 12b shows that the value of L^* is maximized at $\alpha = 0.5$.

Clearly, the value of L^* determines the values of L_{odd} and L_{even}, both of which further determines the ATF-ratios of sensors. Fig. 12c hence reflects that the average power consumption of a WSN falls continuously from $\alpha = 0.15$ until $\alpha = 0.5$, and then begins to increase with some oscillations. Accordingly, we set $\alpha = 0.5$ henceforth. Importantly, Fig. 12c shows that our analysis results are very close to the simulation results, which indeed validate our analysis. The reason why simulation results are slightly higher than analytical results is that in our analysis, we do not count the additional power consumption due to collisions and retransmissions of RTS/CTS packets. Fortunately, thanks to our scalable backoff scheme, such collisions rarely occur.

5.3 Survival Ratio

We use the survival ratio to measure the energy conservation ability of a power saving protocol. In the experiments of Fig. 13, we assume that (i) $\alpha = 0.5$, (ii) $T_{\text{event}}^{\text{sensor}} = 7$, (iii) the total number of sensors is 500, and (iv) the event-to-sink delay requirement is 2 s. From Fig. 9, we can see that under the same cycle length, the ATF-ratio of Queen-MAC is smaller than that of Q-MAC; however, Fig. 13 shows that the lifetime of Queen-MAC is shorter than that of Q-MAC, which is

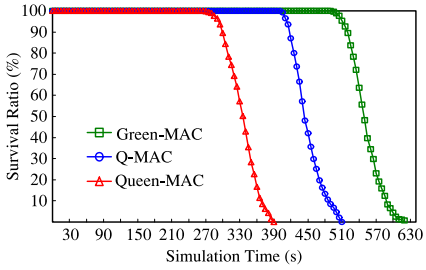

Fig. 13. Survival ratio.

further shorter than that of Green-MAC. The reasons are as follows. Let $\phi_{\mathcal{X}}(C_i)$ denote the ATF-ratio of each sensor in C_i under the power saving protocol $\mathcal{X}$. In Green-MAC, the cycle lengths of sensors are configured according to the event-to-sink delay requirement. In the experiment of Fig. 13, $L_{\text{odd}}^{\text{Green}} = 37$ and $L_{\text{even}}^{\text{Green}} = 38$. Hence $\phi_{\text{Green}}(C_1) = 0.054$ and $\phi_{\text{Green}}(C_2) = 0.0526$. On the other hand, from equations (34), (35), and (36), we can derive that $\phi_{\text{Queen}}(C_i)$ is about two times of $\phi_{\text{Q}}(C_i)$ for all $1 \leq i \leq H_{\max}^{Q} - 1$. Especially, in the experiments of Fig. 13, $\phi_{\text{Q}}(C_1) = 0.07$ and $\phi_{\text{Queen}}(C_1) = 0.133$. Thus Queen-MAC has the shortest lifetime and Green-MAC has the longest lifetime.

5.4 Effect of Event-to-Sink Delay Requirement

This section evaluates the performances of Q-MAC, Queen-MAC, and Green-MAC under various event-to-sink delay requirements. In the experiments of Fig. 14, we assume that (i) $\alpha = 0.5$, (ii) $T_{\text{event}}^{\text{sensor}} = 7$, and (iii) the total number of sensors is 500. From Fig. 14a, we see that as the delay requirement decreases, the delay violation ratio of Green-MAC does not significantly change. This is because as shown in Fig. 14b, the cycle lengths of sensors in Green-MAC are configured according to delay requirements. More heartening, Fig. 14a depicts that when $T_{\text{event}}^{\text{sensor}} \geq 7$, the delay violation ratio of Green-MAC can be no more than 6.7 percent, which is lower than our predefined objective (i.e. $\Phi = 10$ percent). This is because the cycle lengths of sensors in Green-MAC are configured to conquer the *worst* case scenarios (i.e. L^* is derived according to $K_{\min}$ and $H_{\max}$, not according to K_{avg} and H_{avg}), while our simulation results display the performances of Green-MAC under the *average* case scenarios. On the other hand, Fig. 14a shows that the delay violation ratios of Q-MAC and Queen-MAC increase as the delay requirement decreases. This is clearly because the ATF-ratios of sensors in Q-MAC and Queen-MAC are configured according to traffic load and hence fixed. However, to our surprise, the delay violation ratio of Queen-MAC is higher than that of Q-MAC even though from Section 5.3, we know that $\phi_{\text{Queen}}(C_i)$ is about two times of $\phi_{\text{Q}}(C_i)$ for all $1 \leq i \leq H_{\max}^{Q} - 1$. The reasons are as follows. From equations (34) and (35), it is easy to derive that $L^{\text{Queen}} > L_{C_i}^{\text{Q}}$ for all $1 \leq i < H_{\max}^{Q} - 1$. Now, consider the case that in a corona C_i where $i < H_{\max}^{Q} - 1$, the sensors in Q-MAC select one row and one column from a $\sqrt{L_{C_i}^{\text{Q}}} \times \sqrt{L_{C_i}^{\text{Q}}}$ grid as its ATFs, while the sensors in Queen-MAC select k_i *rows* from a $\sqrt{L^{\text{Queen}}} \times \sqrt{L^{\text{Queen}}}$ grid as its ATFs, where $k_i < \sqrt{L^{\text{Queen}}}/2$. In such circumstances, in

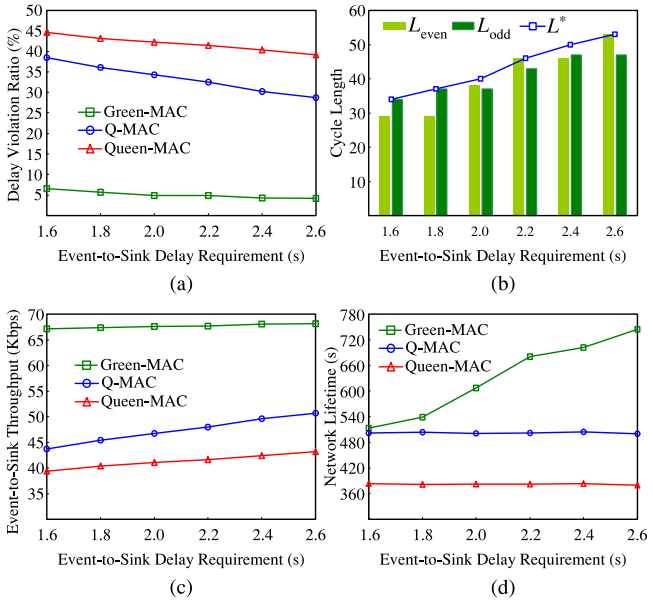

Fig. 14. (a) T_{delay} versus delay violation ratio. (b) Cycle lengths of sensors in Green-MAC. (c) T_{delay} versus event-to-sink throughput. (d) T_{delay} versus network lifetime.

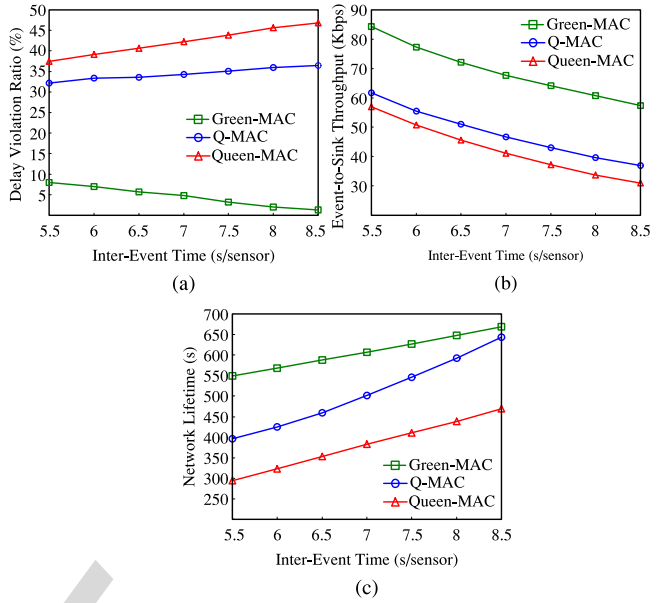

Fig. 15. (a) $T_{\text{event}}^{\text{sensor}}$ versus delay violation ratio. (b) $T_{\text{event}}^{\text{sensor}}$ versus event-to-sink throughput. (c) $T_{\text{event}}^{\text{sensor}}$ versus network lifetime.

Q-MAC, the worst anycast delay (in units of time frame) from C_{i+1} to C_i is about $\sqrt{L_{C_i}^{\text{Q}}}$; in contrast, in Queen-MAC, the worst anycast delay (in units of time frame) from C_{i+1} to C_i can be as high as $\lceil(\sqrt{L^{\text{Queen}}} - k_i)/k_i\rceil \times \sqrt{L^{\text{Queen}}} > L^{\text{Queen}}/(2k_i) > \sqrt{L_{C_i}^{\text{Q}}}$.

Fig. 14c shows that as the delay requirement increases, the event-to-sink throughputs of Q-MAC and Queen-MAC increase, while the event-to-sink throughput of Green-MAC does not significantly change. This just reflects that under the condition that the traffic load of a WSN is fixed, the trends of the event-to-sink throughputs of all protocols are roughly the reverse of the trends of the delay violation ratios of all protocols.

From Fig. 14d, we can see that the lifetimes of Q-MAC and Queen-MAC do not significantly change as the delay requirement increases. This is because in the experiments of Fig. 14, the traffic load of each sensor is fixed. In contrast, the lifetime of Green-MAC grows as the delay requirement increases. This just reflects that as depicted in Fig. 14b, the cycle lengths of sensors in Green-MAC increase with the increasing of delay requirement.

5.5 Effect of Inter-Event Time

This Section evaluates the performances of Q-MAC, Queen-MAC, and Green-MAC under various inter-event time of each sensor (i.e. $T_{\text{event}}^{\text{sensor}}$). In the experiments of Fig. 15, we assume that (i) $\alpha = 0.5$, (ii) the total number of sensors is 500, and (iii) the event-to-sink delay requirement is 2 s. From Fig. 15a, we can see that the delay violation ratios of Q-MAC and Queen-MAC decrease as the value of $T_{\text{event}}^{\text{sensor}}$ decreases. The main reason is that in Q-MAC and Queen-MAC, the ATF ratios of sensors are configured according to traffic load; especially, the heavier the traffic load, the higher the ATF ratios of sensors. On the other hand, Fig. 15a shows that the delay violation ratio of Green-MAC increases as the value of $T_{\text{event}}^{\text{sensor}}$ decreases. This is because when the value of $T_{\text{event}}^{\text{sensor}}$ becomes smaller, it may be more likely to happen that event packets destined for the sink pass through some sensors that have another event packets in their queues. Fortunately, Fig. 15a shows that even when $T_{\text{event}}^{\text{sensor}} = 5.5$ s, the delay violation ratio of Green-MAC is lower than 8.5 percent, which is still lower than our predefined objective (i.e. $\Phi = 10$ percent). This is because in Green-MAC, a backlogged sensor can keep trying to anycast data across multiple time frames (some of which may be originally STFs) until its buffered data is empty. This implies that even though sensors in Green-MAC cannot adjust their cycle lengths, the heavier-loaded sensors can *temporarily and automatically* increase their awake time to quickly relieve the traffic congestion.

From Fig. 15b, we can find that the event-to-sink throughputs of all protocols increase as the value of $T_{\text{event}}^{\text{sensor}}$ decreases. This is because each sensor will generate more event packets when the value of $T_{\text{event}}^{\text{sensor}}$ becomes smaller. Fig. 15b also shows that Green-MAC has higher event-to-sink throughput than the other two protocols, which just reflects that Green-MAC has the lowest delay violation ratio.

Fig. 15c depicts that the lifetimes of all protocols decrease as the value of $T_{\text{event}}^{\text{sensor}}$ decreases. This is because when the value of $T_{\text{event}}^{\text{sensor}}$ becomes smaller, sensors will consume more power to relay increased event packets. In addition, we find that Green-MAC has the longest lifetime. This is because Q-MAC and Queen-MAC configure the ATF-ratios of sensors according to the traffic load, and we have $\phi_{\text{Queen}}(C_1) > \phi_{\text{Q}}(C_1) > \max\{\phi_{\text{Green}}(C_1), \phi_{\text{Green}}(C_2)\}$ in the experiments of Fig. 15c.

5.6 Effect of Sensor Density

In the experiments of this section, we vary the total number N of sensors from 400 to 600; besides, we assume that (i) $\alpha = 0.5$, (ii) $T_{\text{event}}^{\text{sensor}} = 7$, and (iii) the event-to-sink delay requirement is 2 s. Since the radius of the simulated WSN region is fixed, this parameter (i.e. total number of sensors) reflects the sensor density of a WSN. Further, since the value

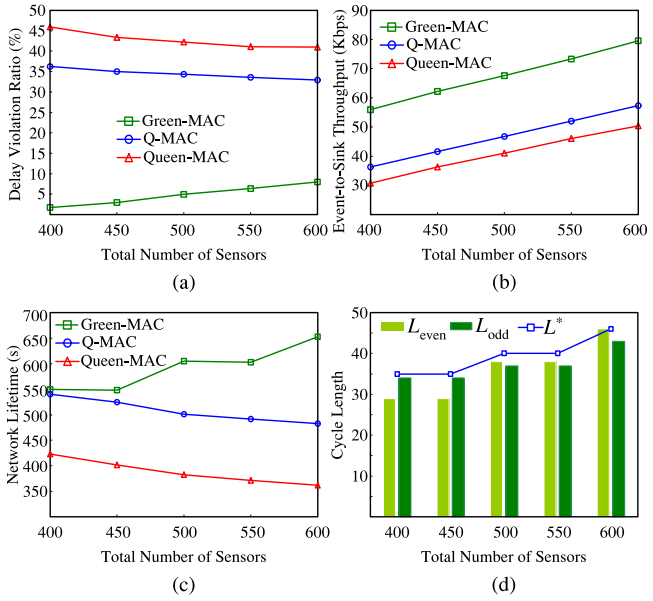

Fig. 16. (a) N versus delay violation ratio. (b) N versus event-to-sink throughput. (c) N versus network lifetime. (d) Cycle lengths of sensors in Green-MAC.

of $T_{\text{event}}^{\text{sensor}}$ is fixed and $T_{\text{event}}^{\text{WSN}} = T_{\text{event}}^{\text{sensor}}/N$, the experiments of Fig. 16 is equivalent to examine the effect of the traffic load of a WSN. On the other hand, when the value of N is fixed, varying the value of $1/T_{\text{event}}^{\text{sensor}}$ is also equivalent to varying the traffic load of a WSN. Thus compared with Figs. 15 and 16, we can see that with regard to the delay violation ratio and event-to-sink throughput, the performance trends of all protocols under various values of N are similar to the reverse of the performance trends of all protocols under various values of $T_{\text{event}}^{\text{sensor}}$. The most interesting part of the experiments in this section is Fig. 16c, which shows that as the total number of sensors increases, the lifetimes of Q-MAC and Queen-MAC decrease, while the lifetime of Green-MAC can increase. The reasons are as follows. We know that the ATF-ratios of sensors in Q-MAC and Queen-MAC are configured according to the traffic load. Especially, in the experiments of Fig. 16, when the value of N becomes larger, the traffic load of a WSN will become heavier, which will lead to larger values of $\phi_{\text{Queen}}(C_1)$ and $\phi_{\text{Q}}(C_1)$. Thus Q-MAC and Queen-MAC have shorter lifetimes in a denser WSN. In contrast, the ATF-ratios of sensors in Green-MAC are configured according to the delay requirement. Especially, the ATF-ratio of a sensor also depends on the minimum next-hop group size, which will become larger when the sensor density increases. Thus Green-MAC has a longer lifetime in a denser WSN. Note that Fig. 16c shows that the lifetime of Green-MAC grows in a ladder shape as the delay requirement increases. This is because as depicted in Fig. 16d, the values of $L_{\text{odd}}^{\text{Green}}$ and $L_{\text{even}}^{\text{Green}}$ remain unchanged when the total number of sensors increases from 400 to 450 and from 500 to 550, respectively.

6 Conclusion

Since sensors are generally battery-powered, it is vital to design a good power saving protocol to prolong the lifetime of a WSN. Especially, in a corona-based WSN, local traffic is mainly anycast; thus the authors of [6] proposed a beacon-free power saving protocol, called Q-MAC, in which each sensor wakes up in the ATFs corresponding to a pre-configured grid quorum. Further, based on the principle that a WSN can work well even by only ensuring the overlap of ATFs between sensors in neighboring coronas, the authors of [12] designed the Queen-MAC, which can achieve only half the ATF-ratio of Q-MAC under the same cycle length condition.

However, in terms of ATF-ratio and configurability, the performances of both Q-MAC and Queen-MAC are far from optimal. This motivates us to design the Green-MAC protocol, in which the feasible cycle patterns of a sensor are constructed by using the generalized Chinese remainder theorem. Importantly, Green-MAC achieves the minimum ATF-ratio and maximized configurability for a corona-based WSN. To the best of our knowledge, Green-MAC is the first power saving protocol for WSNs where the ATF-ratio of *every* sensor with a cycle length L can be only $O(1/L)$, which strikingly breaks the long-term quorum limit $O(1/\sqrt{L})$ established in 2005 [15]. To illuminate the power of configurability, we propose an ATF-ratio configuration scheme to configure the cycle length for sensors in each corona such that the event-to-sink delay requirement can be satisfied with high probability while the power consumption of a WSN can be minimized. Through extensive simulations, we have not only validated our theoretical analysis but also shown that Green-MAC significantly outperforms Q-MAC and Queen-MAC in terms of ATF-ratio, configurability, network lifetime, delay violation ratio, and event-to-sink throughput.

Acknowledgments

The authors would like to thank the editor and the reviewers for their valuable comments that helped to improve the quality of this paper. This work was financially supported by the Ministry of Science and Technology of Taiwan, Republic of China, under grant MOST 103-2221-E-110-052. Dr. Zi-Tsan Chou is the corresponding author.

References

[1] G. Anastasi, M. Conti, M. D. Francesco, and A. Passarella, "Energy conservation in wireless sensor networks: A survey," *Ad Hoc Netw.*, vol. 7, no. 3, pp. 537–568, May 2009.

[2] L. Atzori, A. Iera, and G. Morabito, "The internet of things: A survey," *Comput. Netw.*, vol. 54, no. 15, pp. 2787–2805, Oct. 2010.

[3] B. Buchli, F. Sutton, and J. Beutel, "GPS-equipped wireless sensor network node for high-accuracy positioning applications," in *Proc. Eur. Conf. Wireless Sens. Netw.*, Feb. 2012, pp 179–195.

[4] M. Buettner, G. V. Yee, E. Anderson, and R. Han, "X-MAC: A short preamble MAC protocol for duty-cycled wireless sensor networks," in *Proc. Int. Conf. Embedded Netw. Sens. Syst.*, Nov. 2006, pp. 307–320.

[5] C. Cano, B. Bellalta, A. Cisneros, and M. Oliver, "Quantitative analysis of the hidden terminal problem in preamble sampling WSNs," *Ad Hoc Netw.*, vol. 10, pp. 19–36, 2012.

[6] C.-M. Chao and Y.-W. Lee, "A Quorum-based energy-saving MAC protocol design for wireless sensor networks," *IEEE Trans. Veh. Technol.*, vol. 59, no. 2, pp. 813–822, Feb. 2010.

[7] J. Chen, Q. Yu, Y. Zhang, H.-H. Chen, and Y. Sun, "Feedback-based clock synchronization in wireless sensor networks: A control theoretic approach," *IEEE Trans. Veh. Technol.*, vol. 59, no. 6, pp. 2963–2973, Jul. 2010.

[8] Z.-T. Chou, Y.-H. Lin, and R.-H. Jan, "Optimal asymmetric and maximized adaptive power management protocols for clustered ad hoc wireless networks," *IEEE Trans. Parallel Distrib. Syst.*, vol. 22, no. 12, pp. 1961–1968, Dec. 2011.

[9] C. Ding, D. Pei, and A. Salomaa, *Chinese Remainder Theorem: Applications in Computing, Coding, Cryptography*. Singapore: World Scientific, 1996.
[10] J. Du and W. Shi, "App-MAC: An application-aware event-oriented MAC protocol for multimodality wireless sensor networks," *IEEE Trans. Veh. Technol.*, vol. 57, no. 6, pp. 3723–3731, Nov. 2008.
[11] P. Dutta and D. Culler, "Practical asynchronous neighbor discovery and rendezvous for mobile sensing applications," in *Proc. ACM Conf. Embedded Netw. Sens. Syst.*, 2008, pp. 71–84.
[12] G. Ekbatanifard, R. Monsefi, M. H. Yaghmaee M., and S. A. Hosseini S., "Queen-MAC: A quorum-based energy-efficient medium access control protocol for wireless sensor networks," *Comput. Netw.*, vol. 56, no. 8, pp. 2221–2236, May 2012.
[13] S. Ganeriwal, I. Tsigkogiannis, H. Shim, V. Tsiatsis, M. B. Srivastava, and D. Ganesan, "Estimating clock uncertainty for efficient duty-cycling in sensor networks," *IEEE/ACM Trans. Netw.*, vol. 17, no. 3, pp. 843–856, Jun. 2009.
[14] Global Positioning System (GPS). [Online]. Available: http://en.wikipedia.org/wiki/Global_Positioning_System, 2015.
[15] J.-R. Jiang, Y.-C. Tseng, C.-S. Hsu, and T.-H. Lai, "Quorum-based asynchronous power saving protocols for IEEE 802.11 Ad Hoc Networks," *Mobile Netw. Appl.*, vol. 10, nos. 1-2, pp. 169–181, Feb. 2005.
[16] K. Jichang, *Applied Inequalities*, 3rd ed. Beijing, China: Shandong Sci. Technol. Press, 2004.
[17] R. Jurdak, A. G. Ruzzelli, and G. M. P. O'Hare, "Radio sleep mode optimization in wireless sensor networks," *IEEE Trans. Mobile Comput.*, vol. 9, no. 7, pp. 955–968, Jul. 2010.
[18] A. Kandhalu, K. Lakshmanan, and R. R. Rajkumar, "U-connect: A low latency energy-efficient asynchronous neighbor discovery protocol," in *Proc. ACM/IEEE Int. Conf. Inf. Process. Sens. Netw.*, 2010, pp. 350–361.
[19] H. Karl and A. Willig, *Protocols and Architectures for Wireless Sensor Networks*. Hoboken, NJ, USA: Wiley, 2005.
[20] S. Kulkarni, A. Iyer, and C. Rosenberg, "An address-light, integrated MAC and routing protocol for wireless sensor networks," *IEEE/ACM Trans. Netw.*, vol. 14, no. 4, pp. 793–806, Aug. 2006.
[21] J.-C. Kuo and W. Liao, "Hop count distance in flooding-based mobile ad hoc networks with high node density," *IEEE Trans. Veh. Technol.*, vol. 56, no. 3, pp. 1357–1365, May 2007.
[22] A. M. Law and W. David Kelton, *Simulation Modeling and Analysis*, 3rd ed. New York, NY, USA: McGraw-Hill, 2000.
[23] M. J. Miller and N. H. Vaidya, "A MAC protocol to reduce sensor network energy consumption using a wakeup radio," *IEEE Trans. Mobile Comput.*, vol. 4, no. 3, pp. 228–242, May/Jun. 2005.
[24] J. Polastre, J. Hill, and D. Culler, "Versatile low power media access for wireless sensor networks," in *Proc. Int. Conf. Embedded Netw. Sens. Syst.*, Nov. 2004, pp. 95–107.
[25] C. Schurgers, V. Tsiatsis, S. Ganeriwal, and M. Srivastava, "Optimizing sensor networks in the energy-latency-density design space," *IEEE Trans. Mobile Comput.*, vol. 1, no. 1, pp. 70–80, Jan.-Mar. 2002.
[26] Texas Instruments. (2013). CC2420: 2.4 GHz Radio Transceiver [Online]. Available: http://www.ti.com/lit/ds/symlink/cc2420.pdf
[27] S.-L. Wu, P.-C. Tseng, and Zi-Tsan Chou, "Distributed power management protocols for multi-hop mobile ad hoc networks," *Comput. Netw.*, vol. 47, no. 1, pp. 63–85, 2005.
[28] R. Zheng, J. Hou, and L. Sha, "Optimal block design for asynchronous wake-up schedules and its applications in multihop wireless networks," *IEEE Trans. Mobile Comput.*, vol. 5, no. 9, pp. 1228–1242, Sep. 2006.
[29] C. Yuehong, X. Yong, Y. Xiao, and Q. Kaiyu, "Wireless zigbee transceiver for smart meter reading system," in *Proc. IEEE Power Eng. Autom. Conf.*, Sep. 2012, pp. 1–6.
[30] G. Zhou, Y. Wu, T. Yan, T. He, C. Huang, J. A. Stankovic, and T. F. Abdelzaher, "A multifrequency MAC specially designed for wireless sensor network applications," *ACM Trans. Embedded Comput. Syst.*, vol. 9, no. 4, pp. 39:1–39:41, Mar. 2010.

Yu-Hsiang Lin received the BS and MS degree in computer science from Tamkang University and National Chiao Tung University, Taiwan, in 2002 and 2004, respectively. He is currently working toward the PhD degree at the Department of Computer Science, National Chiao Tung University. His research interests include medium access control and mobility management for wireless networks.

Zi-Tsan Chou received the PhD degree in computer science and information engineering from National Taiwan University, Taipei, Taiwan, in 2003. He is currently an associate professor at the Department of Electrical Engineering, National Sun Yat-Sen University, Kaohsiung, Taiwan. His industrial experience includes NEC Research Institute, America, and the Institute for Information Industry, Taiwan. He holds eight United States patents and 11 Taiwan patents in the field of wireless communications. His research interests include medium access control, power management, and quality-of-service control for wireless networks. He is a member of both the IEEE and the IEEE Communications Society.

Chun-Wei Yu received the BS degree in computer science and information engineering from Chang Jung Christian University, Tainan, Taiwan, and the MS degree in electrical engineering from National Sun Yat-Sen University, Kaohsiung, Taiwan, in 2009 and 2014, respectively. His research interests include medium access control and wireless sensor networks.

Rong-Hong Jan received the BS and MS degrees in industrial engineering, and the PhD degree in computer science from National Tsing Hua University, Taiwan, in 1979, 1983, and 1987, respectively. He is currently a retired professor and was previously an associate dean at the Department of Computer Science, National Chiao Tung University. His research interests include wireless networks, mobile computing, distributed systems, network security, and network reliability.